

SG88

NACA TN 2463

# NATIONAL ADVISORY COMMITTEE FOR AERONAUTICS



TECHNICAL NOTE 2463

EXPERIMENTAL INVESTIGATION OF THE PRESSURE  
DISTRIBUTION ABOUT A YAWED CIRCULAR  
CYLINDER IN THE CRITICAL  
REYNOLDS NUMBER RANGE

By William J. Bursnall and Laurence K. Loftin, Jr.

Langley Aeronautical Laboratory  
Langley Field, Va.



Washington

September 1951

AFMDC  
TECHNICAL LIBRARY  
AFL 2811



0065598

1

## NATIONAL ADVISORY COMMITTEE FOR AERONAUTICS

TECHNICAL NOTE 2463

EXPERIMENTAL INVESTIGATION OF THE PRESSURE  
DISTRIBUTION ABOUT A YAWED CIRCULAR  
CYLINDER IN THE CRITICAL  
REYNOLDS NUMBER RANGE

By William J. Bursnall and Laurence K. Loftin, Jr.

## SUMMARY

An experimental investigation has been made of the pressure distribution about a circular cylinder at yaw angles of  $0^\circ$ ,  $15^\circ$ ,  $30^\circ$ ,  $45^\circ$ , and  $60^\circ$  for Reynolds numbers from below the critical value up to about  $5.0 \times 10^5$ . The Reynolds number is based on the cylinder diameter and the component of velocity normal to the leading edge of the cylinder. The Mach number of the flow normal to the cylinder was less than 0.2 for all tests. The results of the investigation indicated that, for the range of Reynolds number near and above the critical value, the flow and force characteristics of a yawed circular cylinder cannot be determined only by the component of flow normal to the axis of the cylinder. For example, the critical Reynolds number decreased from  $3.65 \times 10^5$  for the unyawed cylinder to  $1.00 \times 10^5$  for the  $60^\circ$  yawed cylinder, and the supercritical drag coefficient, based on the flow normal to the leading edge of the cylinder, increased from approximately 0.18 for  $0^\circ$  yaw to approximately 0.74 for  $60^\circ$  yaw. In addition, the localized regions of laminar separation that appeared in the supercritical range of Reynolds number on the unyawed cylinder were not as well defined at yaw angles of  $15^\circ$  and  $30^\circ$  and completely disappeared at yaw angles of  $45^\circ$  and  $60^\circ$ .

## INTRODUCTION

Theoretical investigations of the boundary layer on yawed, infinitely long wings and bodies (references 1 to 3) have shown that the characteristics of laminar boundary layers in planes at right angles to the axis of the body can be considered as independent of the axial flow. For those cases in which regions of turbulent flow exist, the flow in normal planes cannot be shown to be independent of the axial velocity. The degree to which flow fields in planes normal to the axis of yawed, infinite bodies can be approximated by assuming that the normal

and axial components of the flow are independent, however, is not known for those cases in which turbulent flow exists. The accuracy of such an approximation would be expected to depend on such variables as the relative extents of laminar and turbulent flow in the boundary layer, the width of the wake and the degree of turbulence in the wake, the existence and size of localized regions of laminar separation, and the presence and extent of separation of the turbulent boundary layer.

A knowledge of the manner in which an axial velocity influences flow fields involving turbulent motion is important in relation to the analysis of the aerodynamic characteristics of yawed wings and bodies. For this reason, a short experimental investigation has been made of the flow about a circular cylinder at several angles of yaw. A circular cylinder was chosen for two reasons. First, if the presence of an axial component of velocity has important effects on flows involving turbulent motion, such effects would be expected to be large and easily determined for a circular cylinder through the critical range of Reynolds number because wide turbulent wakes, localized regions of laminar separation, and separation of the turbulent boundary layer are present. Second, the characteristics of yawed circular cylinders are of interest in connection with the problem of calculating the forces acting on slender bodies of revolution at angles of attack or yaw. For this particular problem, it is of special interest to learn whether the sharp decrease in drag within a short range of Reynolds number, which is characteristic of unyawed circular cylinders, is independent of the yaw angle when the Reynolds number is based on the normal component of flow.

The investigation, conducted in the Langley low-turbulence pressure tunnel, consisted of measurements of the circumferential pressure distribution on a 2-inch-diameter circular cylinder for yaw angles of  $0^\circ$ ,  $15^\circ$ ,  $30^\circ$ ,  $45^\circ$ , and  $60^\circ$  for Reynolds numbers from below the critical value up to about  $5.0 \times 10^5$ . The Reynolds number is based on the cylinder diameter and the component of velocity normal to the cylinder axis. All tests were made at Mach numbers less than 0.2.

The investigation described herein was suggested by Dr. Arnold M. Kuethe of the Office of Air Research, U. S. Air Force.

## SYMBOLS

$c_{d_n}$	cylinder drag coefficient based on flow normal to axis of cylinder and cylinder diameter $\left( - \int_0^\pi S d(\sin \theta) \right)$
D	diameter of cylinder
$H_{o_n}$	free-stream total pressure normal to axis of cylinder
l	cylinder length between tunnel walls
p	local static pressure
$R_n$	Reynolds number based on cylinder diameter and component of velocity normal to axis of cylinder ( $V_n D / \nu$ )
S	pressure coefficient $\left( \frac{H_{o_n} - p}{\frac{1}{2} \rho V_n^2} \right)$
$U_o$	free-stream velocity
$V_n$	component of velocity in direction normal to axis of cylinder
$\theta$	azimuth angle
$\nu$	free-stream kinematic viscosity
$\rho$	free-stream density
$\psi$	yaw angle

## APPARATUS AND TESTS

Wind tunnel.— The investigation was conducted in the Langley low-turbulence pressure tunnel. The test section measures 3 feet by 7.5 feet and the model, when mounted, completely spanned the 3-foot dimension. A turbulence level of only a few hundredths of a percent is attained in the tunnel test section by means of a large area reduction

through the entrance cone and dense screens in the large section ahead of the entrance cone. Pressurization and evacuation of the tunnel permit a wide variation of the test Reynolds number for any given model. A more complete description of the tunnel may be found in reference 4.

Model.- All tests were made on a 2-inch-diameter circular brass tube fitted with a static-pressure orifice at each of three spanwise stations (6 inches apart) but at the same azimuth angle. The model extended through the tunnel walls and was connected to a drive system which permitted rotation of the cylinder about its axis. The pressure could therefore be measured at any desired point on the circumference of the cylinder. The surface of the model was maintained in an aerodynamically smooth condition by polishing with rouge paper.

Figure 1 shows the experimental configuration, defines the velocities and angles (fig. 1(a)), and shows the location of the static-pressure orifices relative to the tunnel walls for the various yaw angles (fig. 1(b)). Three static-pressure orifices were used for measuring the pressures in order to check the two-dimensionality of the flow. For the various yaw angles, figure 1(b) shows that the locations of the orifices with respect to the wall do not coincide. This condition could not be avoided because of space limitations in the location of the drive mechanism.

The large ratio of cylinder length to diameter ( $\frac{l}{D} = 18$  for  $\psi = 0^\circ$  to  $\frac{l}{D} = 36$  for  $\psi = 60^\circ$ ) was chosen in order that an infinitely long cylinder might be simulated as nearly as possible. Because of the small diameter of the cylinder, the correction to the dynamic pressure resulting from the presence of the tunnel walls was less than one-half of 1 percent. This very small correction was not applied to the data.

Tests.- Circumferential pressure distributions were measured at the three spanwise stations for several Reynolds numbers and for yaw angles of  $0^\circ$ ,  $15^\circ$ ,  $30^\circ$ ,  $45^\circ$ , and  $60^\circ$ . The range of Reynolds number, based on the cylinder diameter and the component of velocity normal to the axis of the cylinder, varied somewhat for each yaw angle but was, in general, from below the critical range to about  $5.0 \times 10^5$ . In order to maintain Mach numbers substantially below the critical value, tank pressures of the tunnel were regulated so that the Mach number of the flow normal to the cylinder was less than 0.2 for all tests.

## RESULTS AND DISCUSSION

Two-dimensionality of data.- Before the effect of yaw on the characteristics of the cylinder is discussed, the question of whether the flow phenomena are uniform across the span of the cylinder for the different yaw angles should be considered. Comparisons for the

different yaw angles of the pressure distributions measured by the three spanwise static orifices in both the subcritical and supercritical ranges of Reynolds number are presented in figure 2. The pressure coefficient employed in figure 2 and succeeding figures is based on the dynamic pressure normal to the axis of the cylinder, and the Reynolds number is based on the cylinder diameter and the component of velocity normal to the cylinder.

An inspection of the data of figure 2 indicates that there are some variations in the pressure distributions as measured by the three spanwise orifices. These variations are most noticeable in the subcritical range and exist even for the case in which the cylinder is unyawed. It is not clear whether these variations result from some interaction between the flow about the ends of the model and the tunnel-wall boundary layer or whether variations of such magnitude would be expected in any so-called two-dimensional flow in which extensive regions of separation and large wakes exist. In any case, the spanwise variations are rather small for all yaw angles and do not appear to form any consistent trend with yaw angle. Consequently, if any end effects are present in the data, such effects are thought to be small and relatively independent of yaw angle. In the following discussion and analysis, results are presented for one spanwise station only; this station is the one closest to the center line of the tunnel in all cases.

Pressure distribution. - The pressure-distribution data obtained for the circular cylinder at yaw angles of  $0^\circ$ ,  $15^\circ$ ,  $30^\circ$ ,  $45^\circ$ , and  $60^\circ$  in the Reynolds number range from below the critical up to about  $5.0 \times 10^5$  are presented in figures 3 to 7. In all cases the pressure distributions were found to be symmetrical about the horizontal diameter of the cylinder; consequently, only half of each distribution is presented. An inspection of the data in figures 3 to 7 indicates a number of points which are perhaps worthy of comment. Consider first the case of zero yaw (fig. 3). The pressure distributions for Reynolds numbers of  $2.00 \times 10^5$  and  $2.45 \times 10^5$  (fig. 3(a)) are typical of those obtained in the low Reynolds number range and show early separation of the boundary layer which implies a large wake. As compared with the pressure distributions for Reynolds numbers below  $3.0 \times 10^5$ , those for Reynolds numbers greater than  $3.5 \times 10^5$  (fig. 3(b)) are characterized by high peak negative pressures and irregularities in the pressure-distribution diagram just behind the minimum point, followed by a relatively long pressure recovery before separation of the turbulent boundary layer occurs. The "flat" in the pressure distributions for the Reynolds numbers of  $4.54 \times 10^5$  and  $5.96 \times 10^5$  and the subsequent steep pressure recovery indicate the presence of a localized region of laminar separation; that is, laminar separation followed by reattachment of the turbulent boundary layer (reference 5). If the Reynolds number were increased to a sufficiently high value in the supercritical range, transition would be expected to move ahead of the position at which laminar separation would have occurred had

the boundary layer remained laminar, and under such circumstances, a localized region of laminar separation would not exist. In order to simulate a Reynolds number of such magnitude, a 0.024-inch-diameter wire was placed 0.5 inch ahead of the model as a means of inducing early transition. The resulting pressure distribution is shown in figure 3(b) and indicates that no localized region of laminar separation is present. The data of references 6 and 7 for circular cylinders also indicate the presence of localized regions of laminar separation of the type discussed in reference 5, although the existence of such regions was not clearly recognized at the time of publication.

A comparison of the measured pressure distributions at the lowest Reynolds number for each yaw angle is presented in figure 8 and shows that, in general, the subcritical pressure distribution is relatively insensitive to yaw except for the rearward part of the cylinder at all yaw angles and the entire circumference of the cylinder at the yaw angle of  $60^\circ$ . These discrepancies can be explained by the fact that, although the laminar boundary layer over the forward part of the cylinder is presumably independent of the cross flow according to references 1 to 3, the character of the relatively large turbulent wake which has an important influence on the pressure distribution is not independent of the cross flow.

An inspection of the measured pressure distributions for the different yaw angles (figs. 4 to 7) indicates that a gradual change takes place in the distributions through and beyond the critical range as the yaw angle is increased. Although the localized regions of separation still exist at  $15^\circ$  and  $30^\circ$  (figs. 4 and 5), they do not appear as well-defined as at zero yaw. Increasing the yaw angle to  $45^\circ$  and  $60^\circ$  (figs. 6 and 7) results in the complete disappearance of the localized region of separation. These results indicate that the formation and behavior of localized regions of laminar separation are not independent of cross flow, at least for circular cylinders.

The value of the peak negative pressure coefficient in the super-critical range of Reynolds number (figs. 3(b), 4(b), 5(b), 6(b), and 7(b)) is seen to be relatively insensitive to yaw angle except for  $45^\circ$  yaw, in which case the peak pressure is substantially lower than for the other yaw angles. The reason for this reduction in minimum pressure coefficient at  $45^\circ$  yaw is not entirely clear. The point at which the turbulent boundary layer separates is seen to be about the same for yaw angles of  $0^\circ$ ,  $15^\circ$ , and  $30^\circ$  but to move forward by relatively large amounts for yaw angles of  $45^\circ$  and  $60^\circ$  with an accompanying increase in the negative pressure in the wake.

Drag.- The drag coefficients corresponding to the various yaw angles have been calculated by integration of the measured pressure distributions about the circumference of the cylinder and are presented in figure 9

as a function of Reynolds number. The critical Reynolds number defined as the Reynolds number at which the drag decreases rapidly is approximately  $3.65 \times 10^5$  for the unyawed cylinder. This value is much higher than that obtained in earlier investigations such as those reported in references 7 to 9. The lower value of the critical Reynolds number in the earlier tests is probably due to the higher turbulence levels of the wind tunnels. The present results compare favorably, however, with those of a flight investigation (reference 10) in which a value of approximately  $3.0 \times 10^5$  was found for the critical Reynolds number.

An examination of the data of figure 9 indicates that, although a large decrease in the drag coefficient with Reynolds number occurs for all yaw angles except for the case of  $60^\circ$  yaw, this decrease becomes much more gradual as the yaw angle is increased. Although a critical Reynolds number for the yaw angles between  $0^\circ$  and  $60^\circ$  cannot be defined, the Reynolds number at which the drag begins to decrease generally appears to decrease with increasing yaw angle. For the yaw angle of  $60^\circ$  the decrease in drag with increasing Reynolds number is very abrupt and the corresponding critical Reynolds number is about  $1.00 \times 10^5$  as compared to  $3.65 \times 10^5$  for the unyawed cylinder. If the Reynolds number were based on the stream velocity and the chord length in the stream direction, the critical Reynolds number for the  $60^\circ$  yawed cylinder would be about  $4.00 \times 10^5$ . For this particular case at least, the critical Reynolds number seems to be more nearly independent of yaw if this Reynolds number is based on the stream flow rather than the normal flow. The normal component of the drag force is seen to decrease somewhat with increase in yaw angle in the subcritical region (fig. 9) except for the  $60^\circ$  yawed cylinder. The very large increase of the supercritical drag coefficient with yaw angle is clearly shown in figure 10. The data of figures 9 and 10 show that the drag characteristics of a circular cylinder cannot be related only to the Reynolds number based on normal velocity component for Reynolds numbers in and above the critical range.

#### CONCLUDING REMARKS

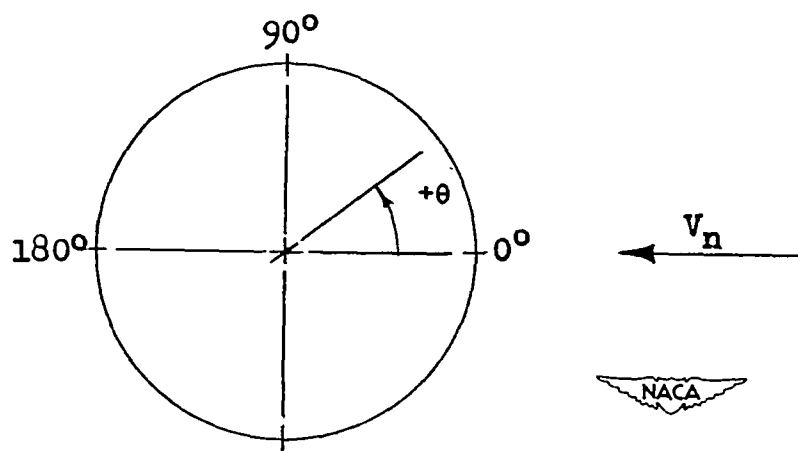
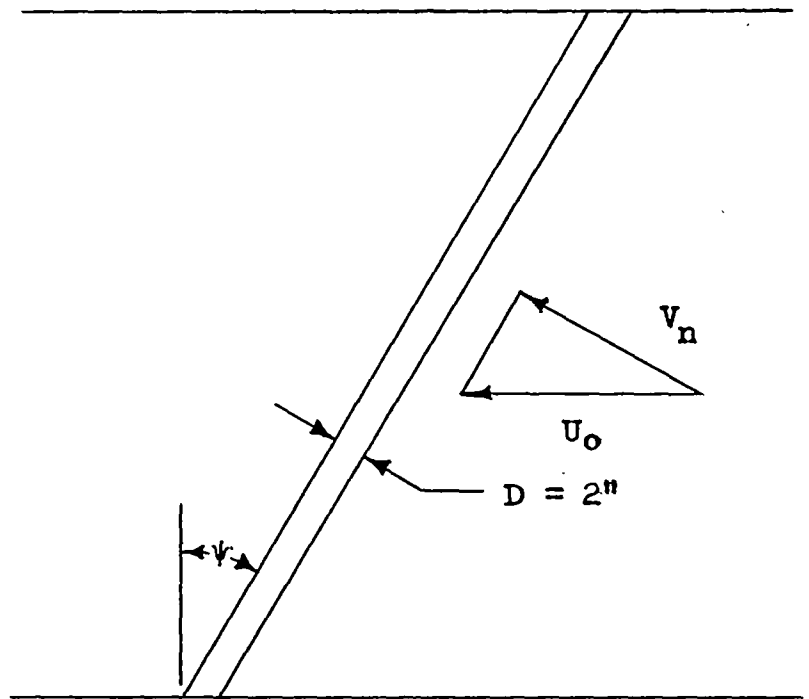
An experimental investigation has been made of the pressure distribution about a circular cylinder at yaw angles of  $0^\circ$ ,  $15^\circ$ ,  $30^\circ$ ,  $45^\circ$ , and  $60^\circ$  for Reynolds numbers ranging from below the critical value up to about  $5.0 \times 10^5$ . The Reynolds number is based on the diameter of the cylinder and the component of velocity normal to the axis of the cylinder. The Mach number of the flow normal to the cylinder was less than 0.2 for all tests. The results of the investigation indicated that for the range of Reynolds number near and above the critical the flow and force characteristics of a yawed circular cylinder cannot be determined only by the component of flow normal to the axis of the cylinder. For example, the critical Reynolds number decreased from  $3.65 \times 10^5$  for the unyawed

cylinder to  $1.00 \times 10^5$  for the  $60^\circ$  yawed cylinder, and the supercritical drag coefficient, based on the flow normal to the leading edge of the cylinder, increased from a value of approximately 0.18 for  $0^\circ$  yaw to approximately 0.74 for  $60^\circ$  yaw. In addition, the localized regions of laminar separation that appeared in the supercritical range of Reynolds number on the unyawed cylinder were not as well-defined at yaw angles of  $15^\circ$  and  $30^\circ$  and completely disappeared at yaw angles of  $45^\circ$  and  $60^\circ$ .

Langley Aeronautical Laboratory  
National Advisory Committee for Aeronautics  
Langley Field, Va., June 22, 1951

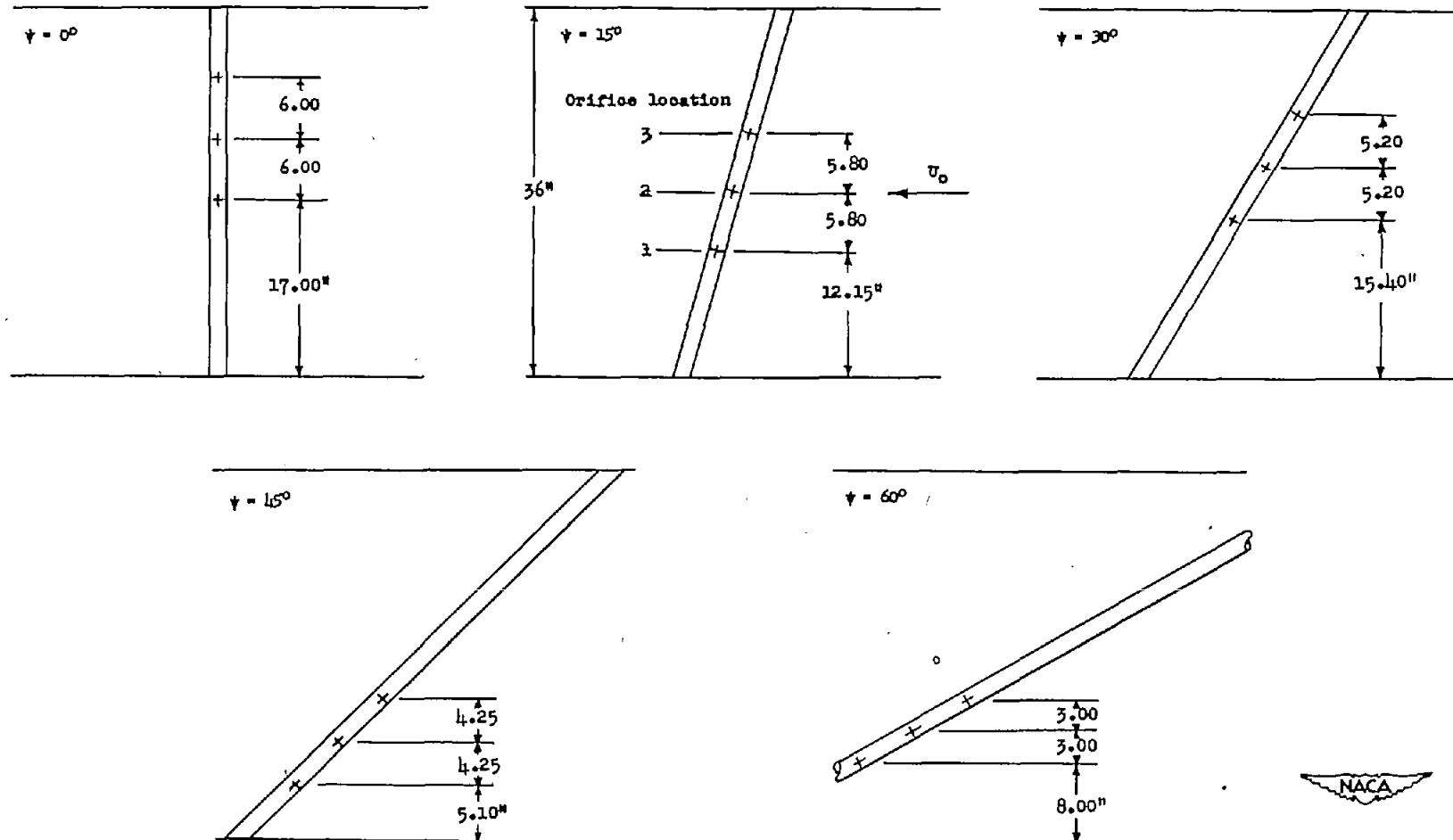
## REFERENCES

1. Sears, W. R.: The Boundary Layer of Yawed Cylinders. *Jour. Aero. Sci.*, vol. 15, no. 1, Jan. 1948, pp. 49-52.
2. Wild, J. M.: The Boundary Layer of Yawed Infinite Wings. *Jour. Aero. Sci.*, vol. 16, no. 1, Jan. 1949, pp. 41-45.
3. Jones, Robert T.: Effects of Sweep-Back on Boundary Layer and Separation. NACA Rep. 884, 1947.
4. Von Doenhoff, Albert E., and Abbott, Frank T., Jr.: The Langley Two-Dimensional Low-Turbulence Pressure Tunnel. NACA TN 1283, 1947.
5. Bursnall, William J., and Loftin, Laurence K., Jr.: Experimental Investigation of Localized Regions of Laminar-Boundary-Layer Separation. NACA TN 2338, 1951.
6. Fage, A.: The Air Flow around a Circular Cylinder in the Region where the Boundary Layer Separates from the Surface. R. & M. No. 1179, British A.R.C., 1928.
7. Fage, A., and Falkner, V. M.: Further Experiments on the Flow around a Circular Cylinder. R. & M. No. 1369, British A.R.C., 1931.
8. Fage, A.: The Drag of Circular Cylinders and Spheres at High Values of Reynolds Number. R. & M. No. 1370, British A.R.C., 1930.
9. Wieselsberger, C.: New Data on the Laws of Fluid Resistance. NACA TN 84, 1922.
10. Stephens, A. V.: Drag of Circular Cylinders in Flight. R. & M. No. 1892, British A.R.C., 1940.



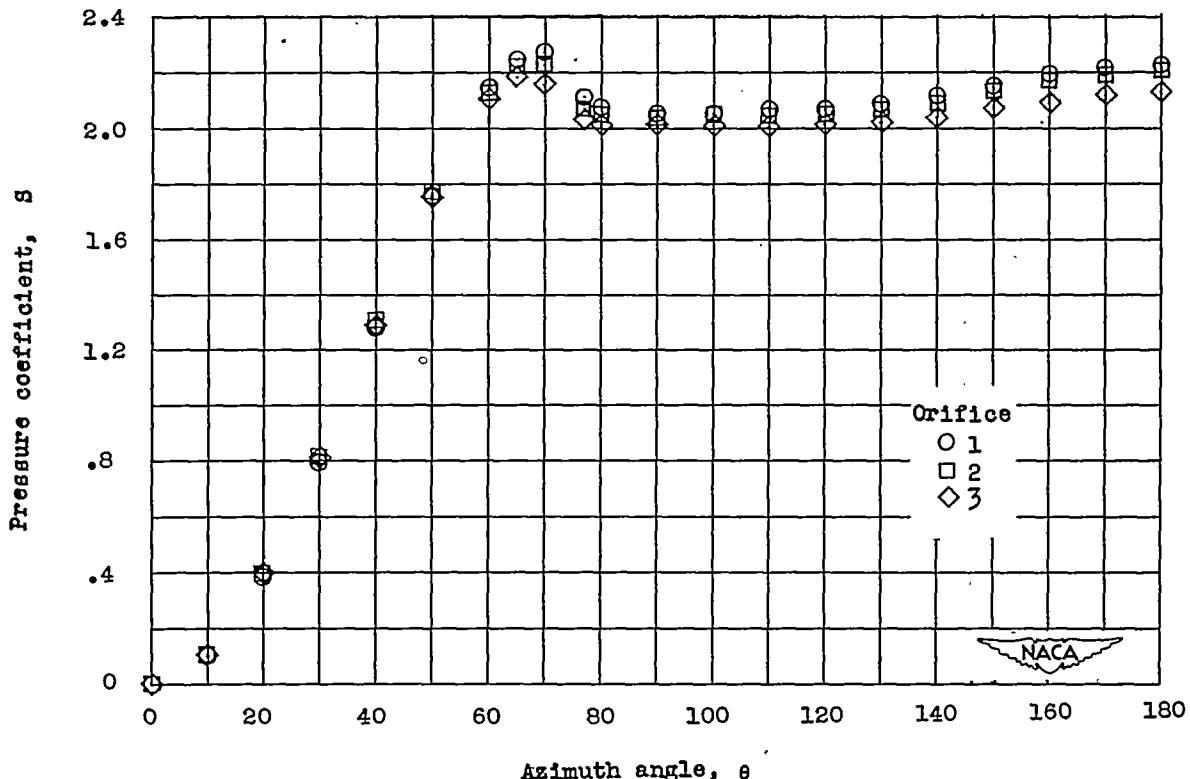
(a) Definition of velocities and angles.

Figure 1.- Experimental configuration.



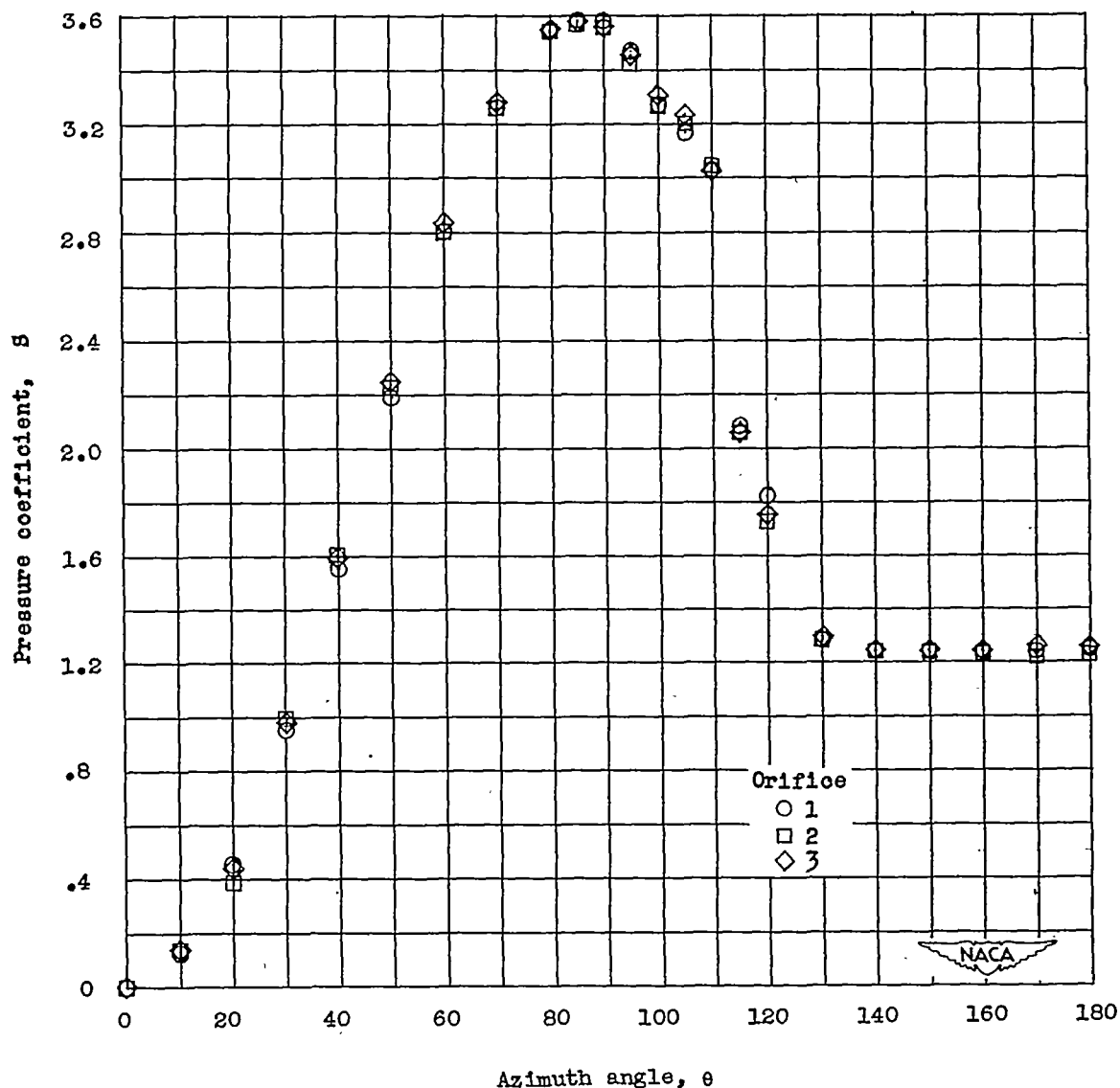
(b) Location of the static-pressure orifices in relation to the tunnel walls.

Figure 1.- Concluded.



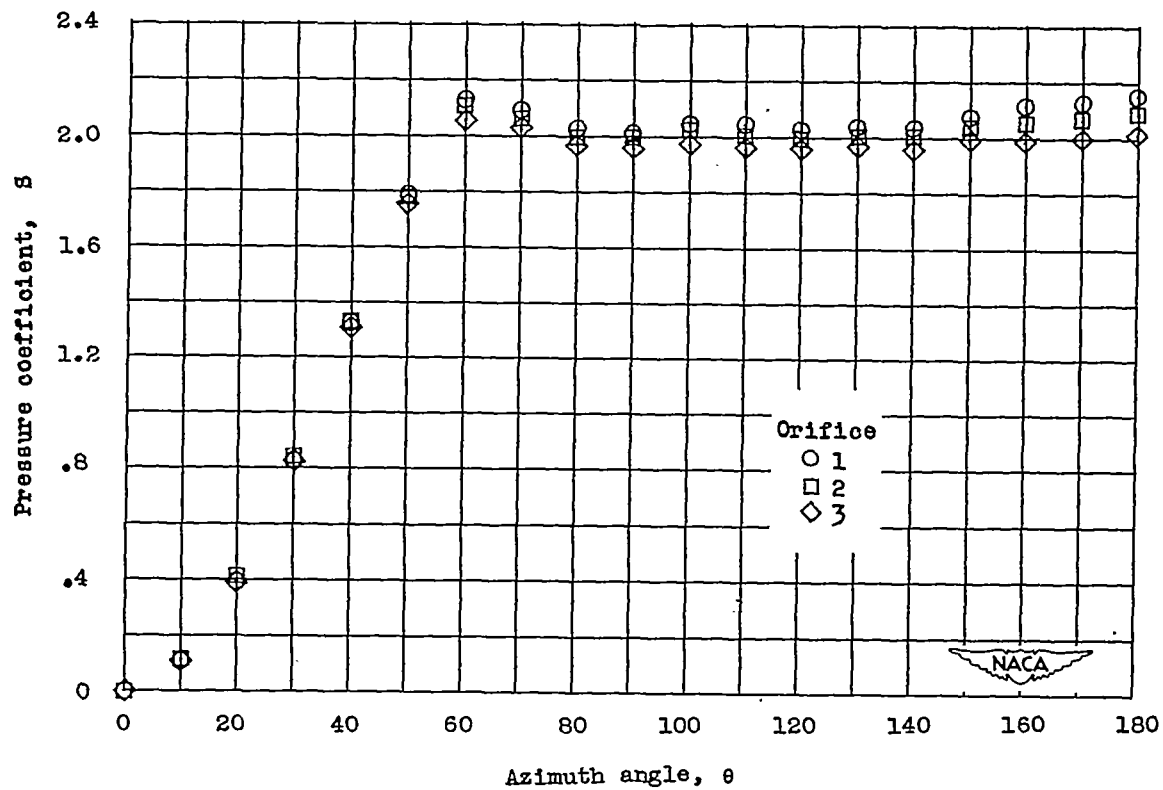
(a)  $\psi = 0^\circ$ ;  $R_n = 2.00 \times 10^5$  (subcritical).

Figure 2.- Comparison of circumferential pressure distributions measured at three spanwise stations 6 inches apart on a 2-inch-diameter circular cylinder at several angles of yaw.



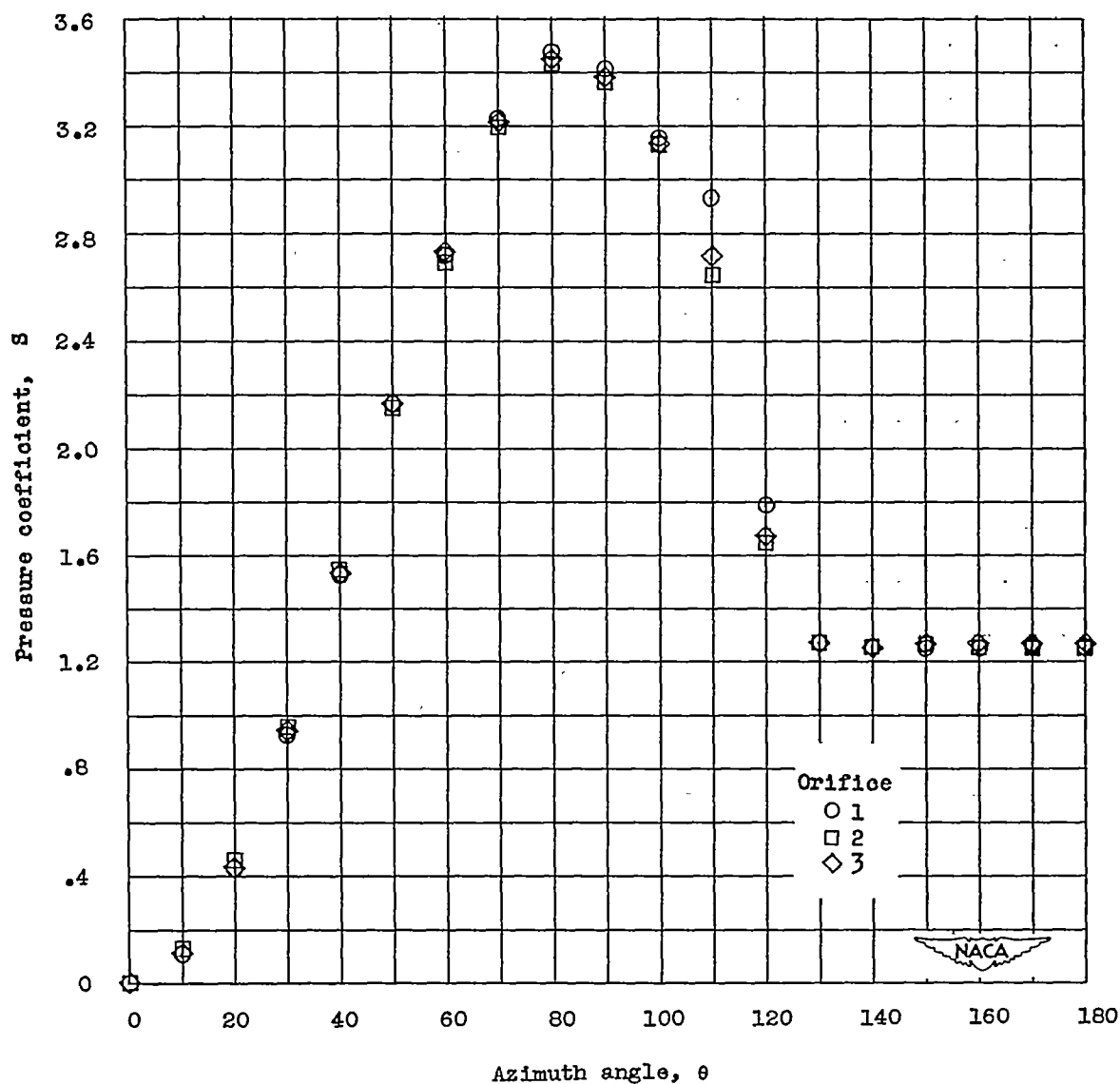
(b)  $\psi = 0^\circ$ ;  $R_n = 3.77 \times 10^5$  (supercritical).

Figure 2.- Continued.



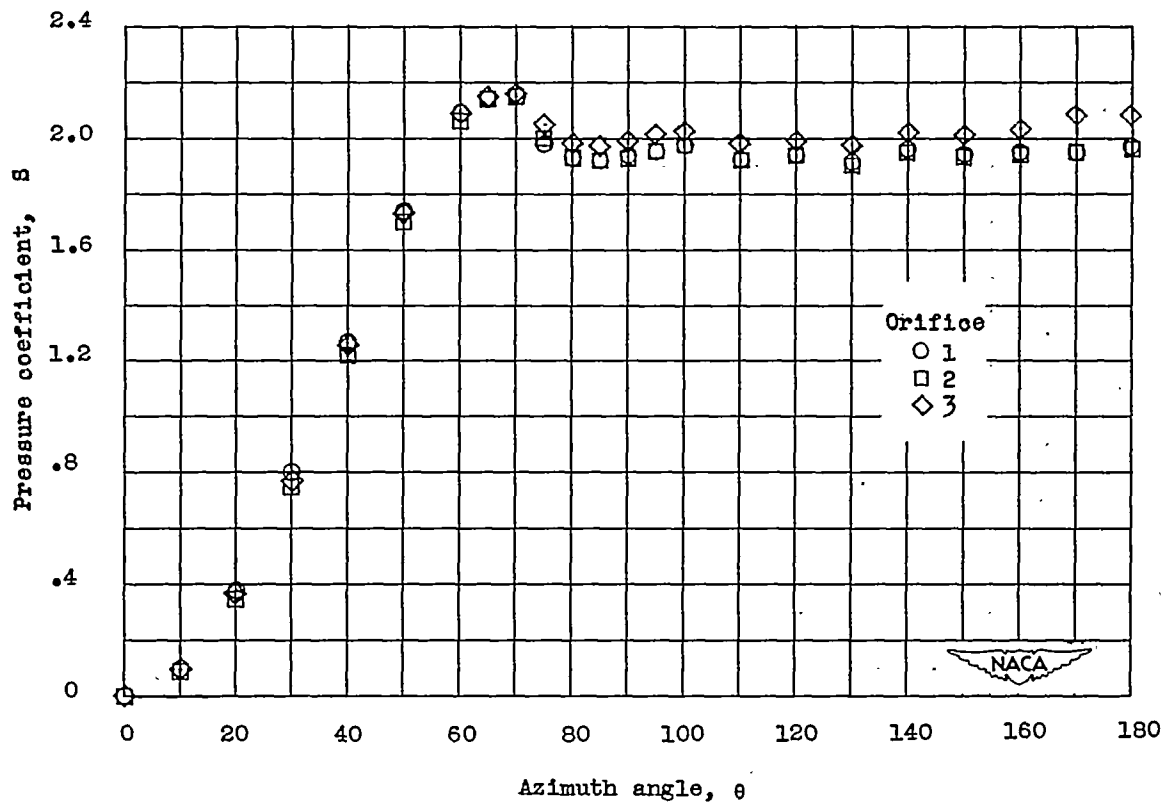
(c)  $\psi = 15^\circ$ ;  $R_n = 2.01 \times 10^5$  (subcritical).

Figure 2.- Continued.



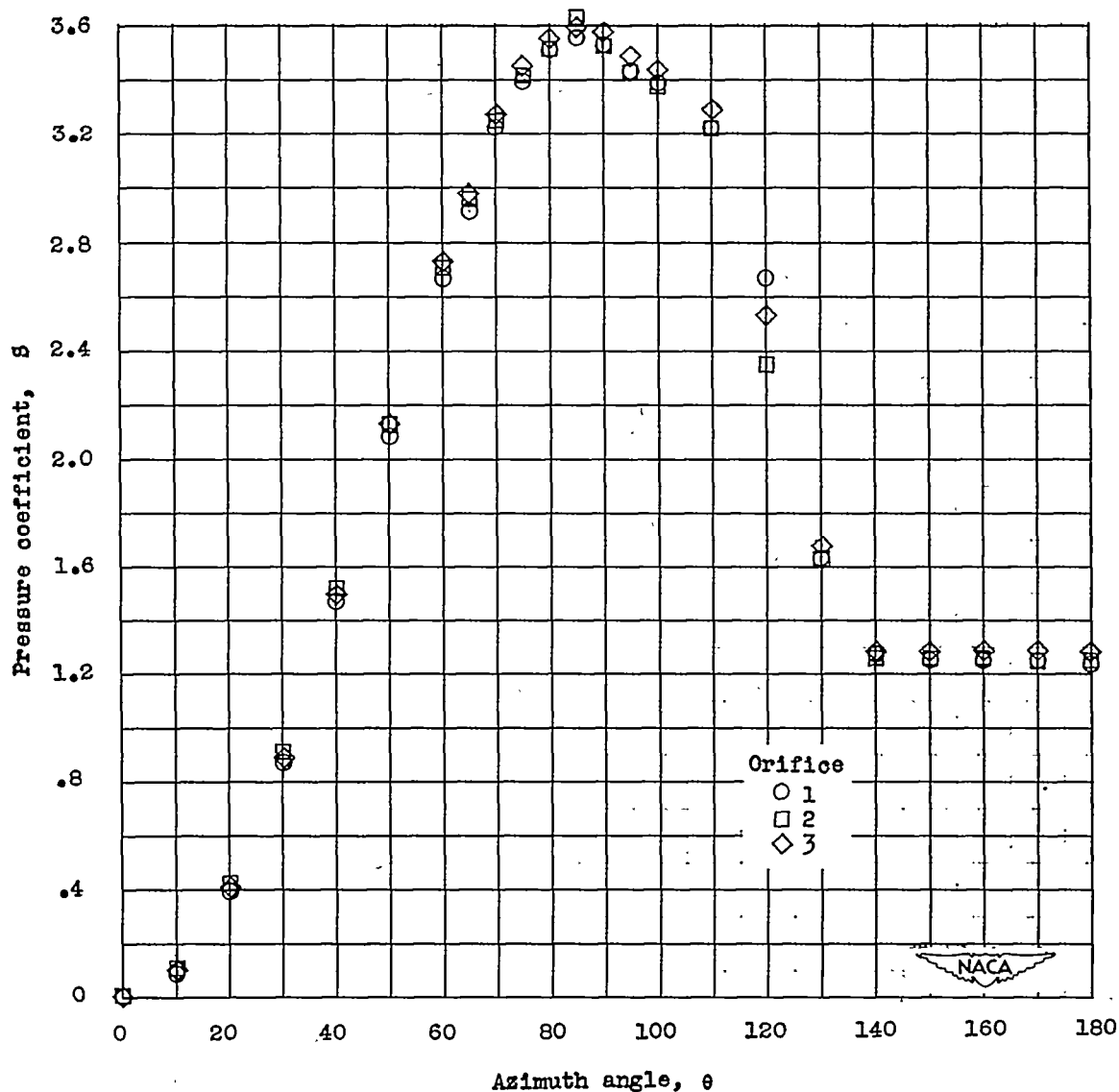
(d)  $\psi = 15^\circ$ ;  $R_n = 3.67 \times 10^5$  (supercritical).

Figure 2.- Continued.



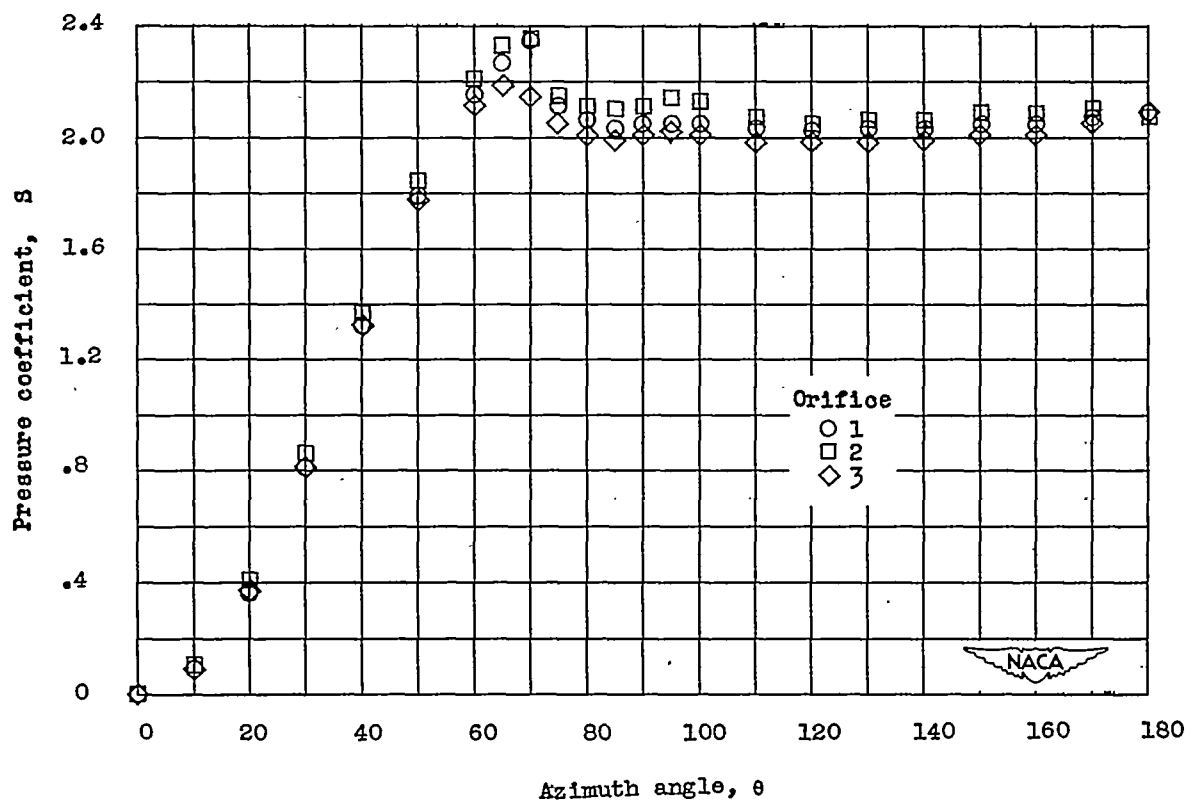
(e)  $\psi = 30^\circ$ ;  $R_n = 1.99 \times 10^5$  (subcritical).

Figure 2.- Continued.



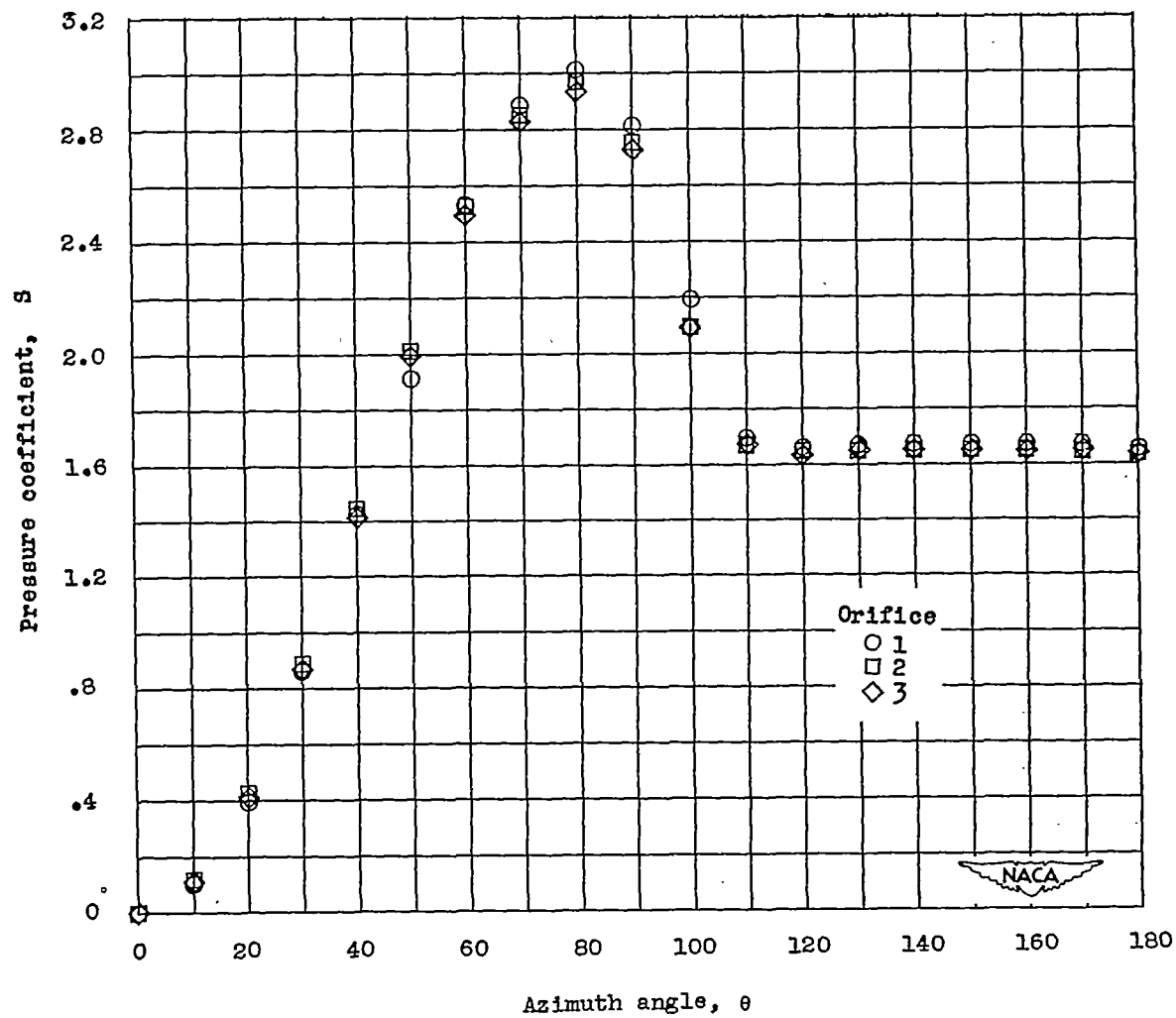
(f)  $\psi = 30^\circ$ ;  $R_n = 3.98 \times 10^5$  (supercritical).

Figure 2.- Continued.



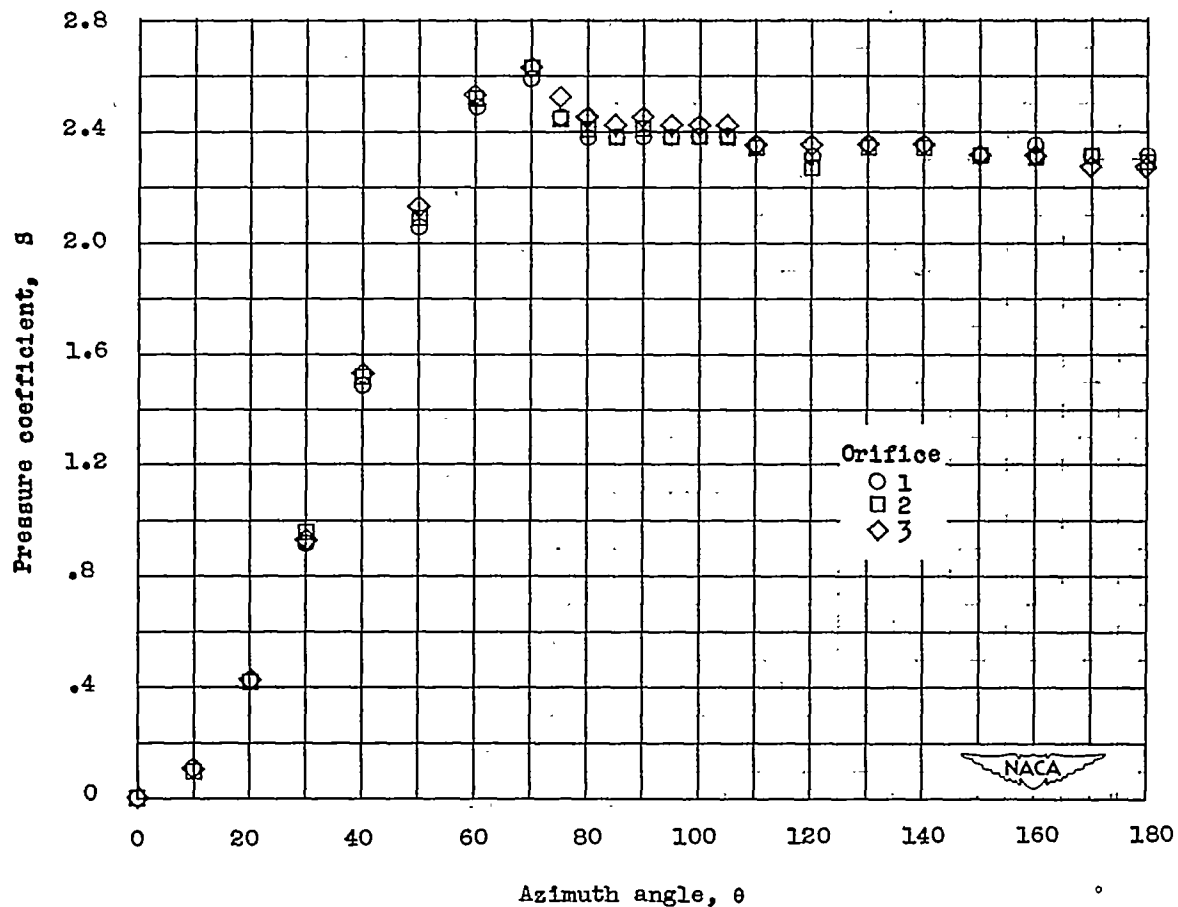
(g)  $\psi = 45^\circ$ ;  $R_n = 1.76 \times 10^5$  (subcritical).

Figure 2.- Continued.



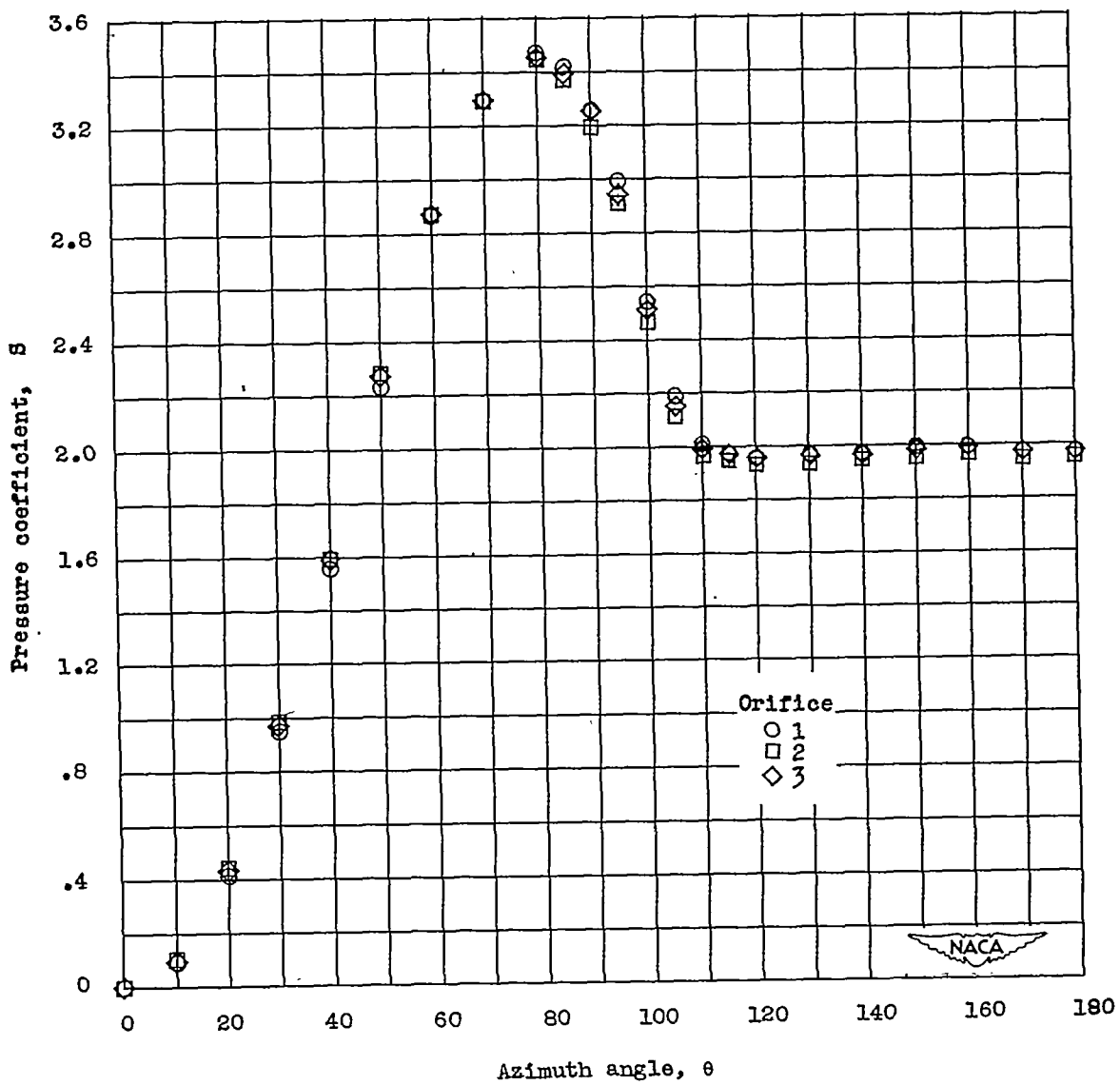
(h)  $\psi = 45^\circ$ ;  $R_n = 3.52 \times 10^5$  (supercritical).

Figure 2.- Continued.



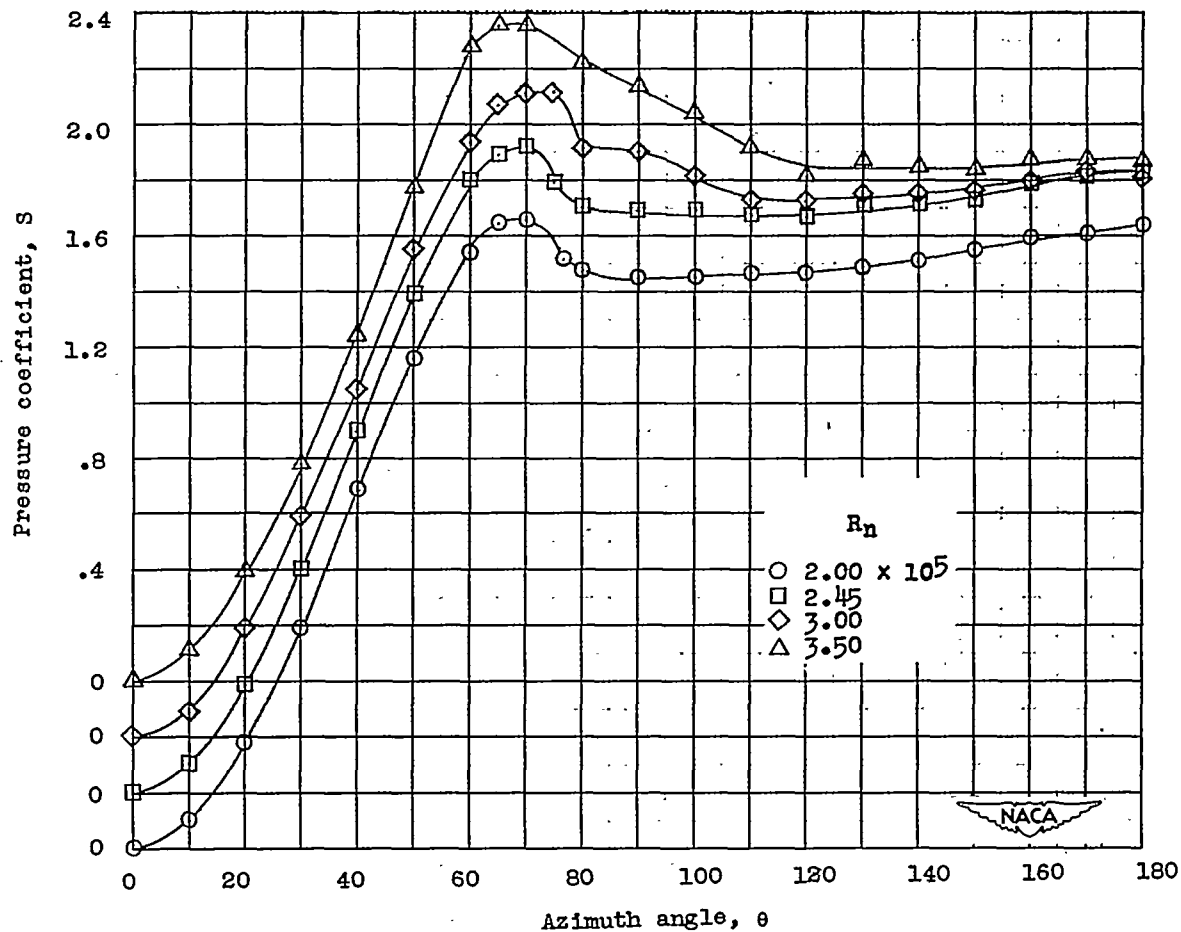
(i)  $\psi = 60^\circ$ ;  $R_n = 1.02 \times 10^5$  (subcritical).

Figure 2.- Continued.



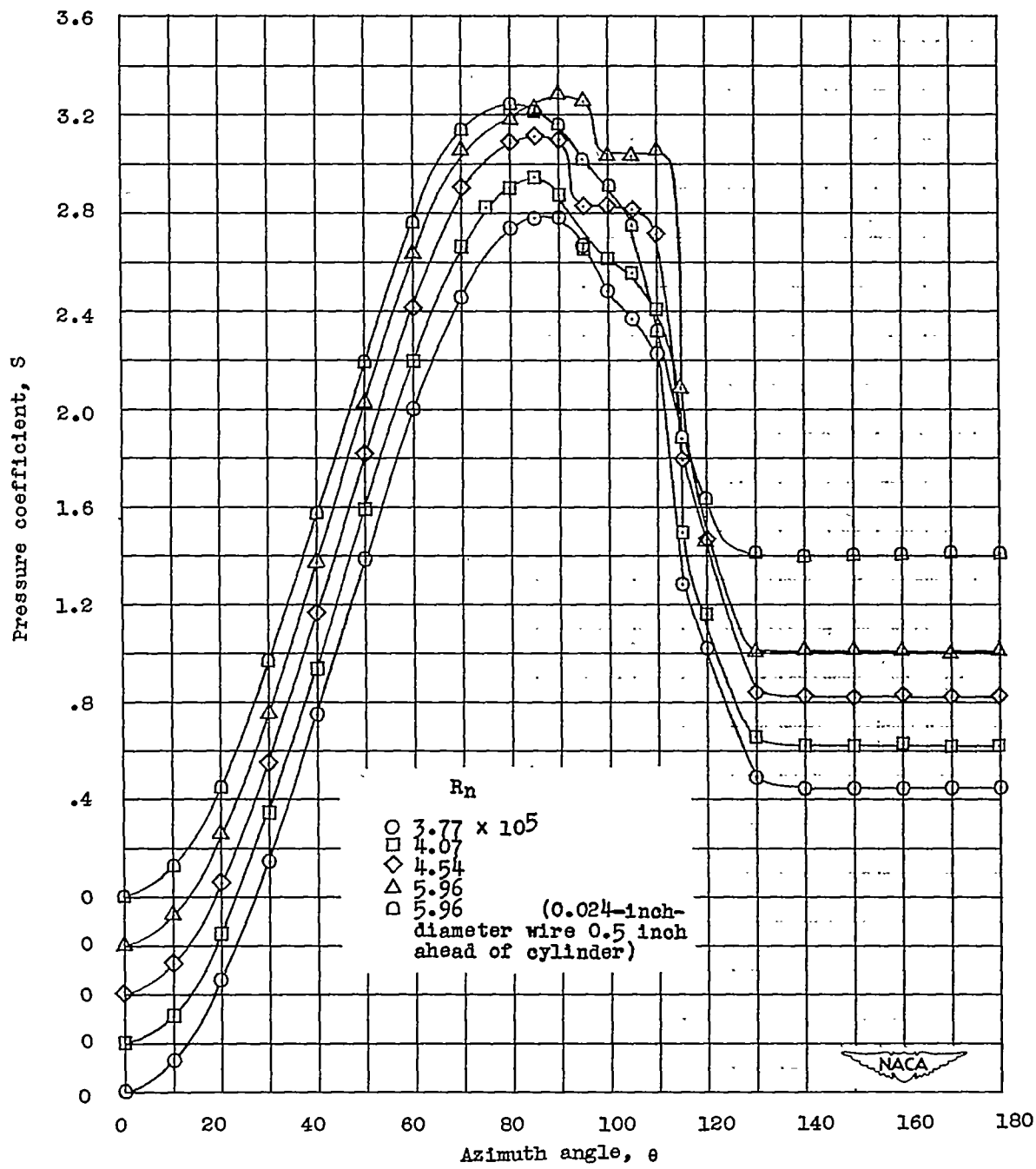
(j)  $\psi = 60^\circ$ ;  $R_n = 3.45 \times 10^5$  (supercritical).

Figure 2.- Concluded.



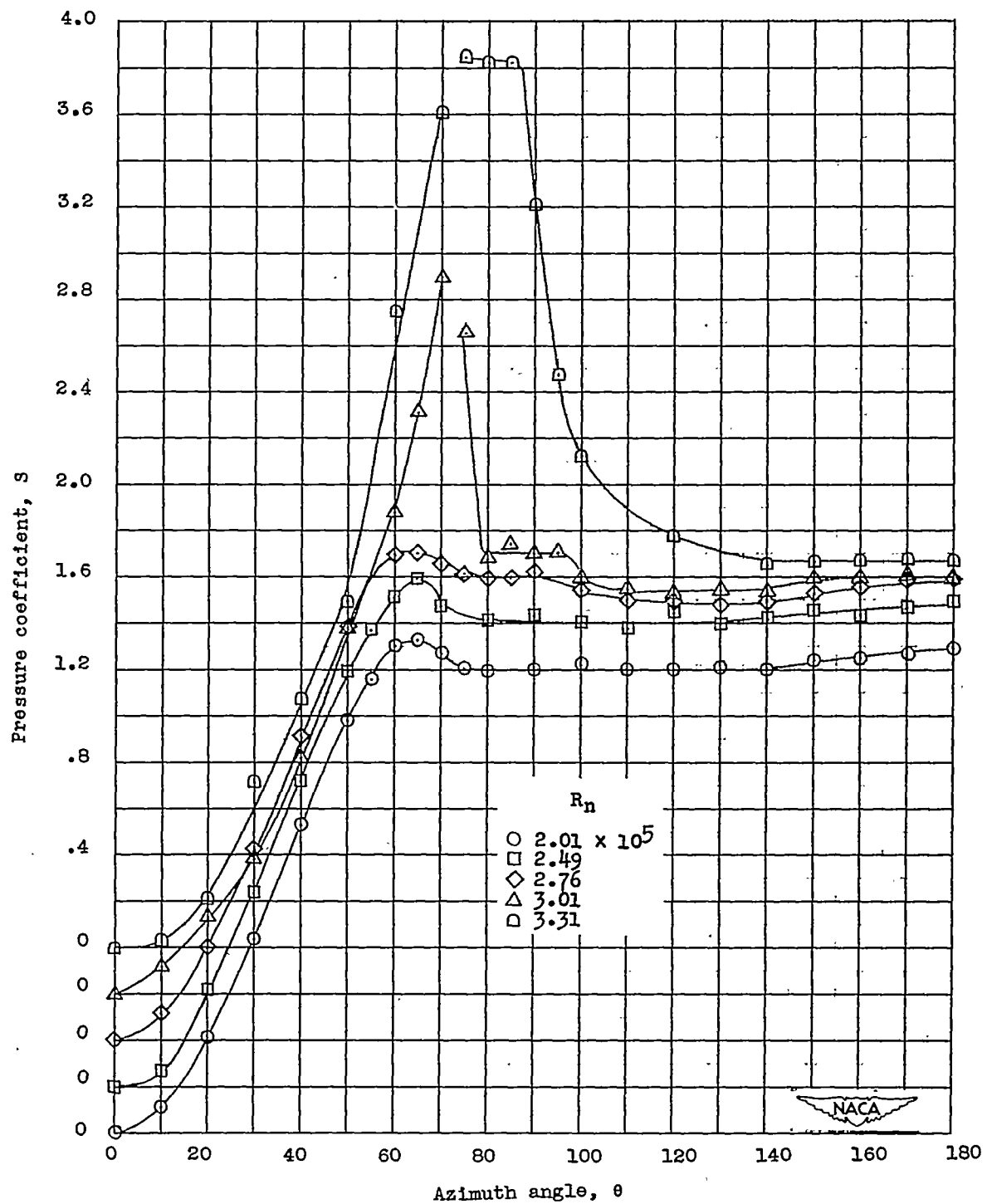
(a)  $R_n = 2.00 \times 10^5$  to  $R_n = 3.50 \times 10^5$ .

Figure 3.- Circumferential pressure distribution of a 2-inch-diameter unyawed circular cylinder at several Reynolds numbers.



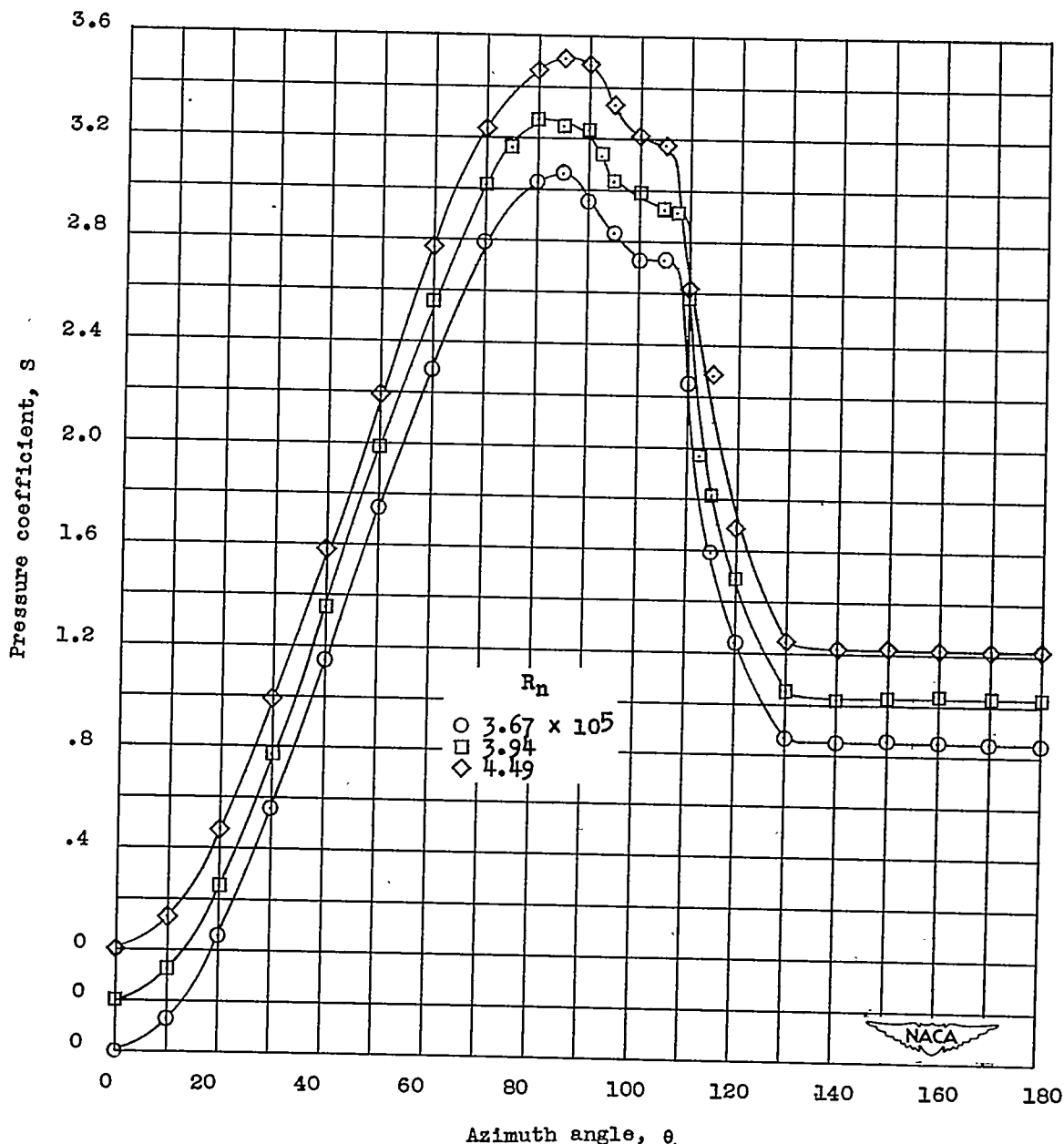
(b)  $R_n = 3.77 \times 10^5$  to  $R_n = 5.96 \times 10^5$ .

Figure 3.- Concluded.



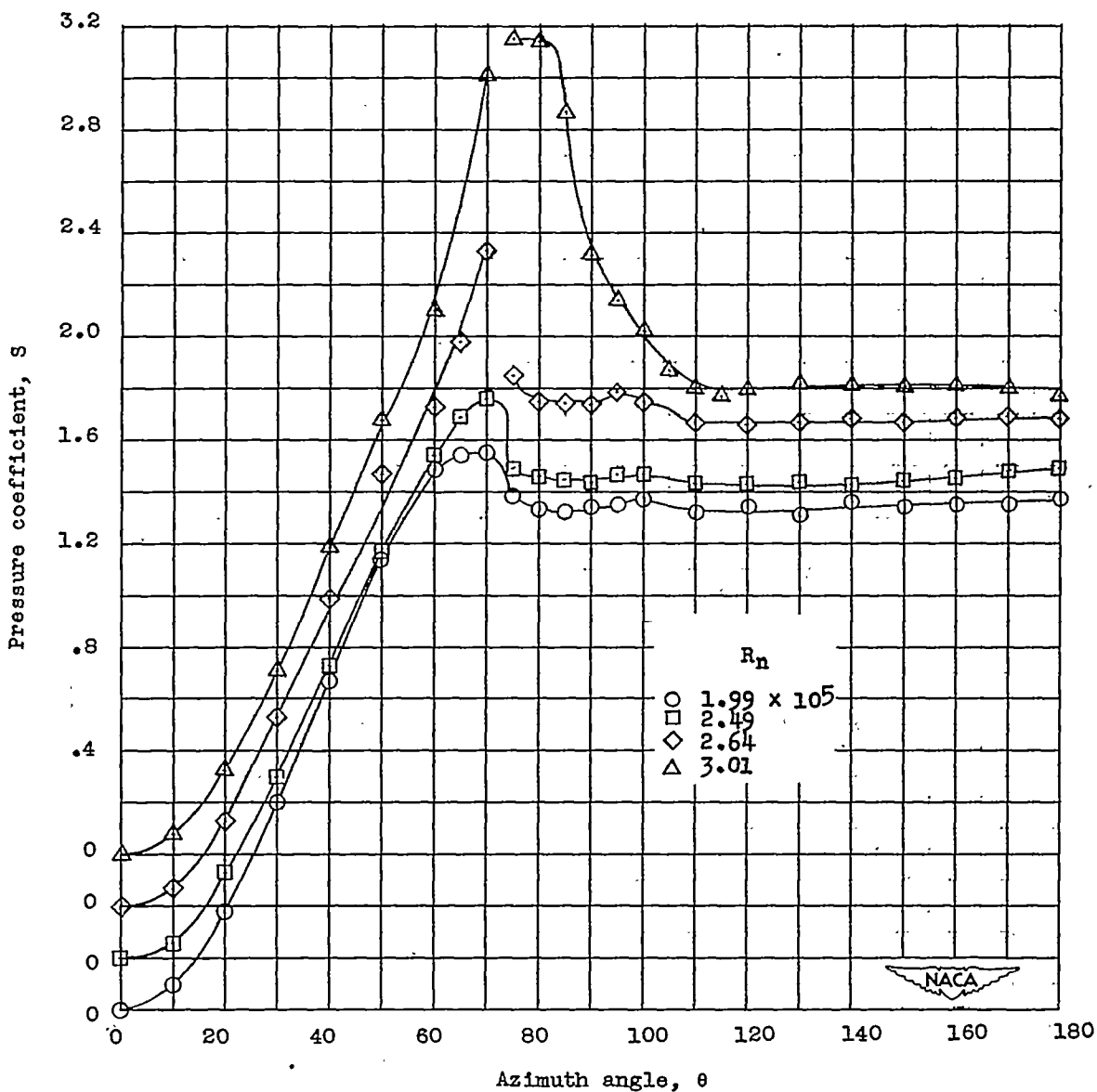
(a)  $R_n = 2.01 \times 10^5$  to  $R_n = 3.31 \times 10^5$ .

Figure 4.- Circumferential pressure distributions at several Reynolds numbers of a 2-inch-diameter circular cylinder yawed  $15^\circ$ .



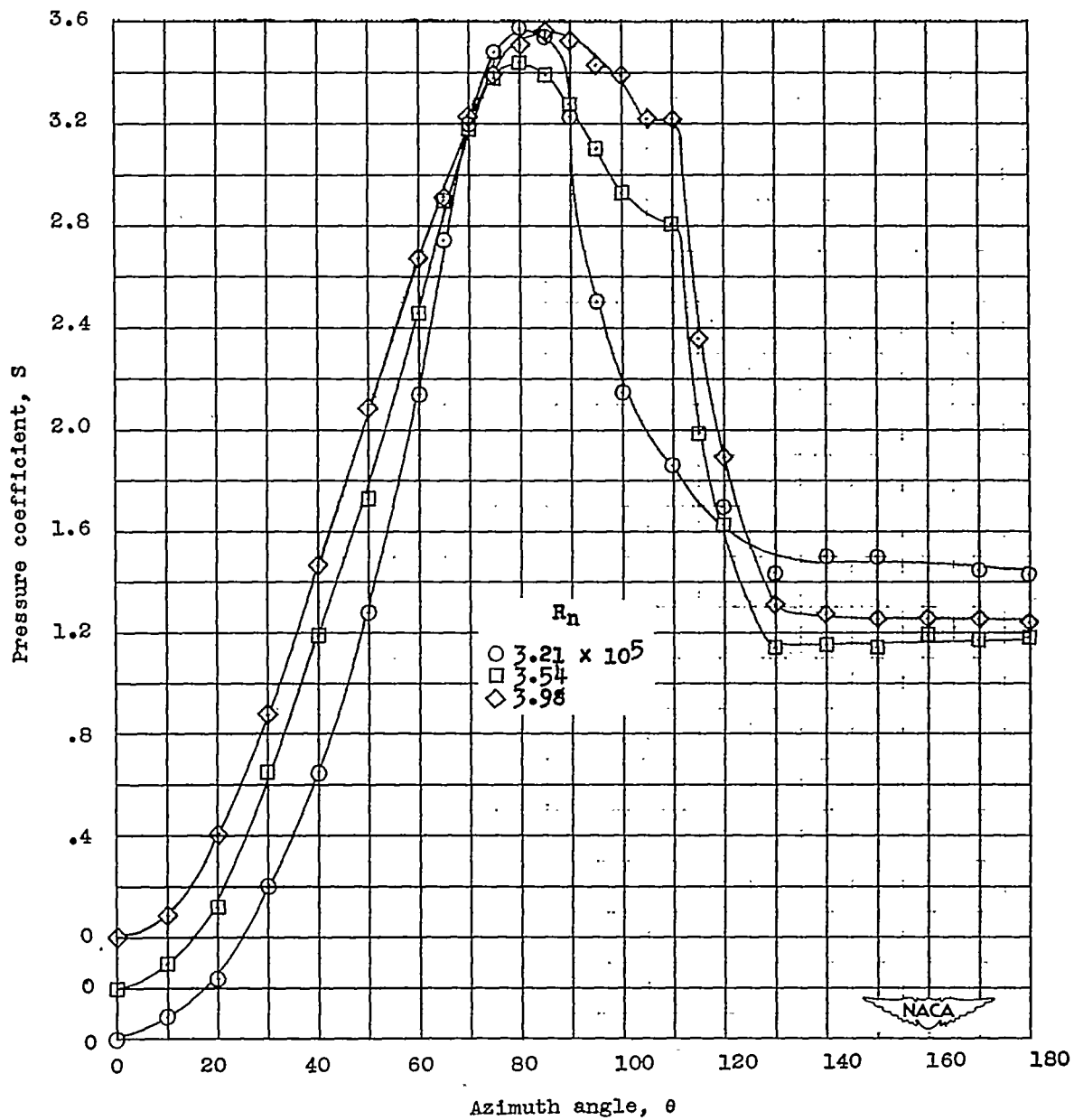
(b)  $R_n = 3.67 \times 10^5$  to  $R_n = 4.49 \times 10^5$ .

Figure 4.- Concluded.



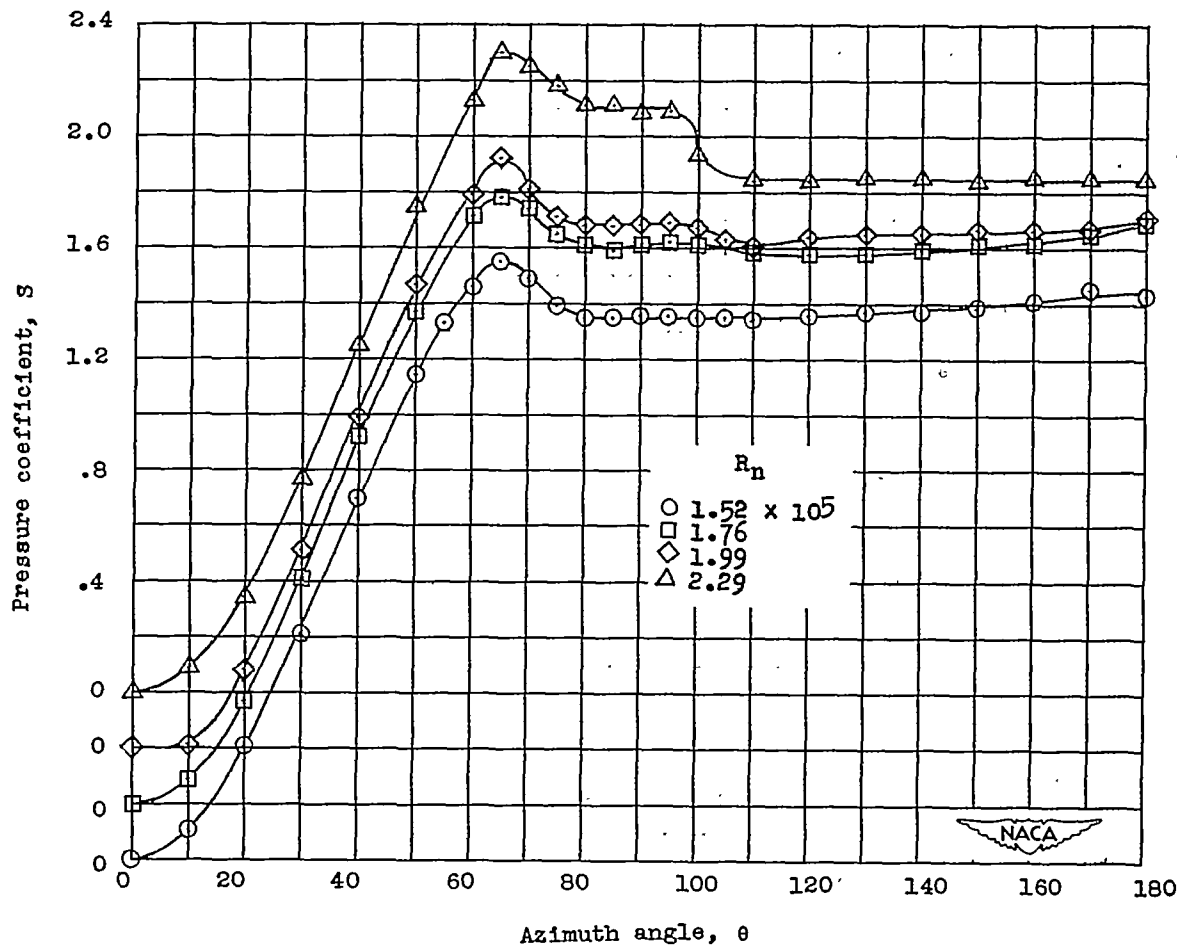
(a)  $R_n = 1.99 \times 10^5$  to  $R_n = 3.01 \times 10^5$ .

Figure 5.- Circumferential pressure distributions at several Reynolds numbers of a 2-inch-diameter circular cylinder yawed  $30^\circ$ .



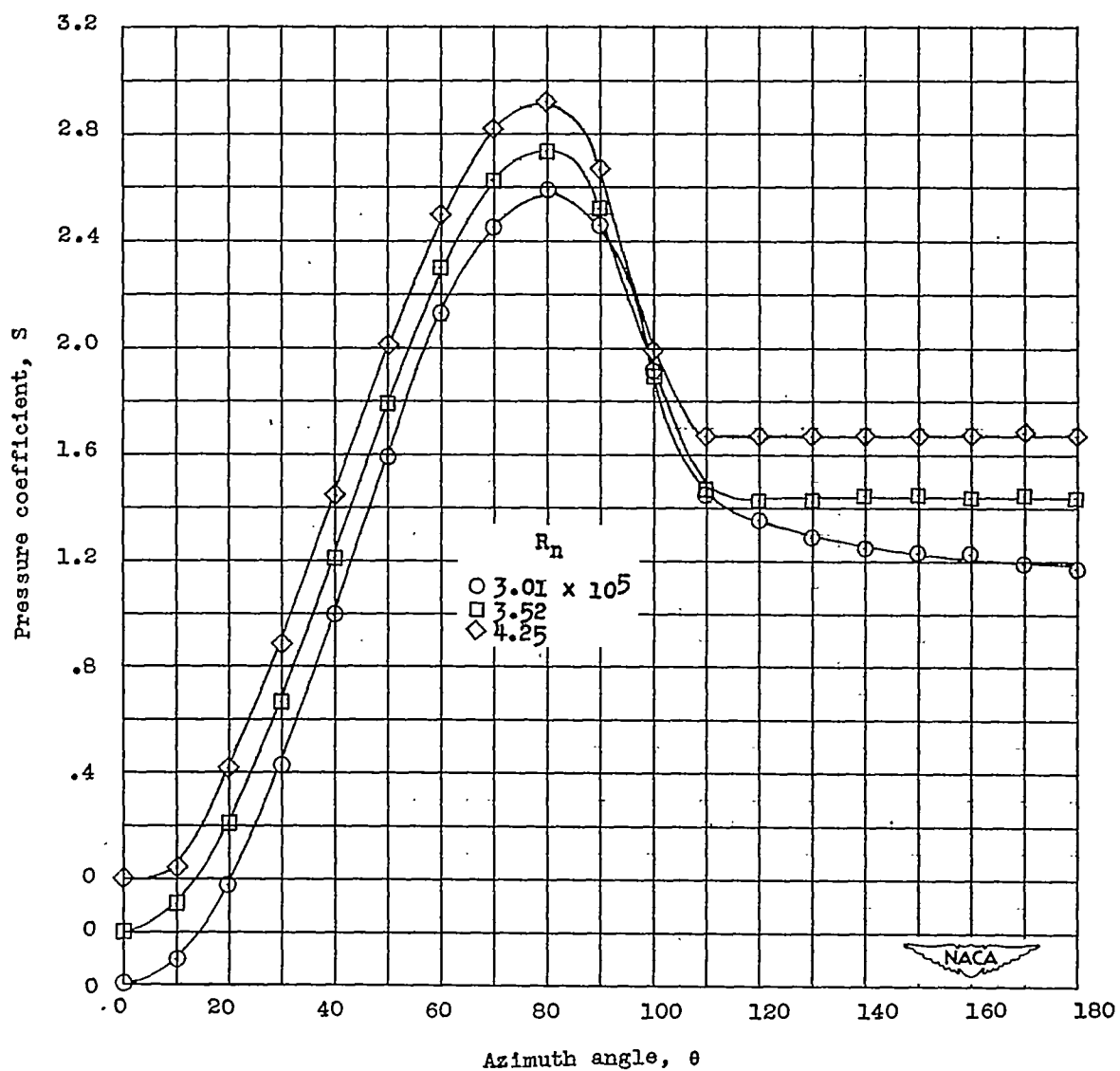
(b)  $R_n = 3.21 \times 10^5$  to  $R_n = 3.98 \times 10^5$ .

Figure 5.- Concluded.



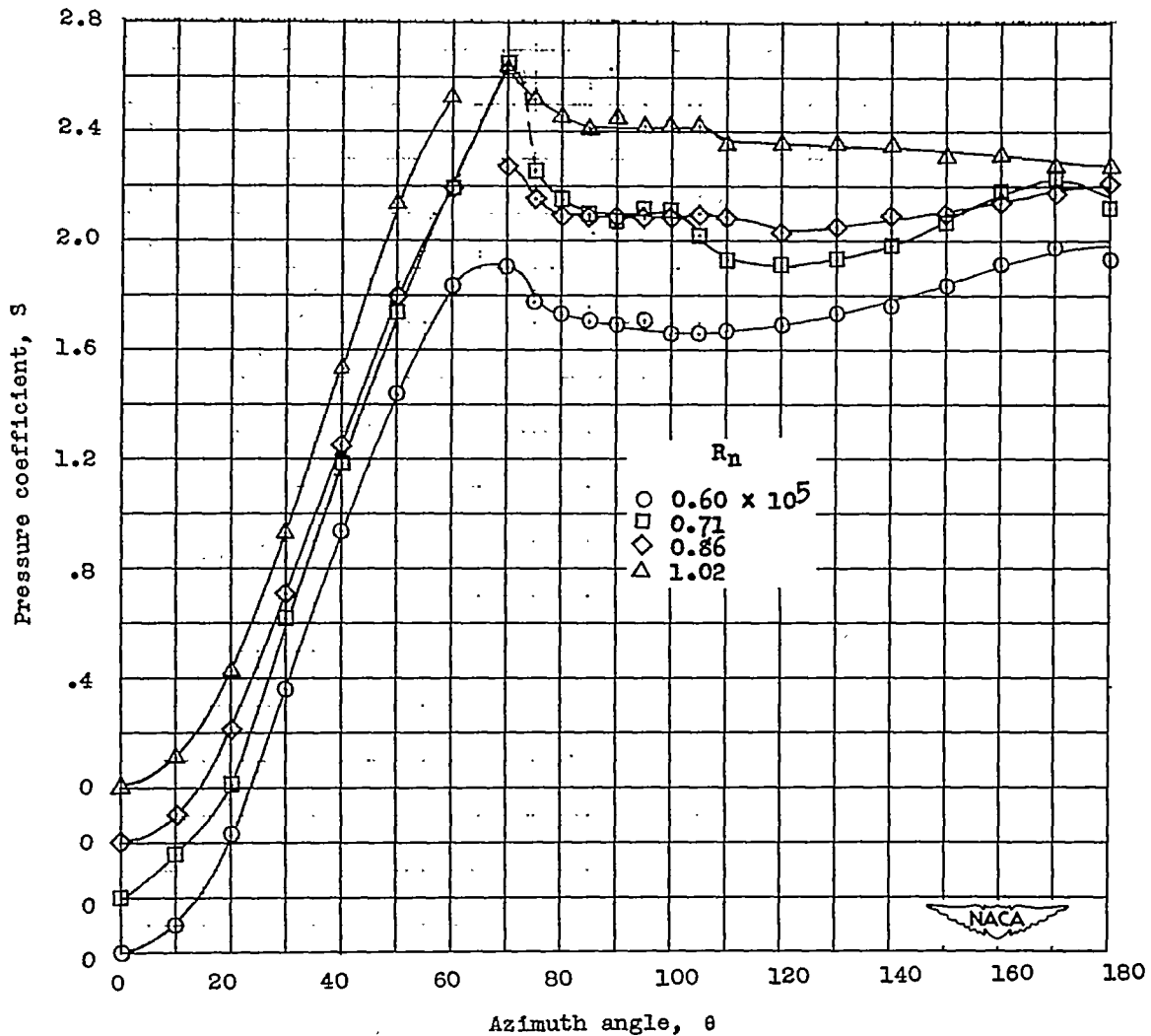
(a)  $R_n = 1.52 \times 10^5$  to  $R_n = 2.29 \times 10^5$ .

Figure 6.- Circumferential pressure distributions at several Reynolds numbers of a 2-inch-diameter circular cylinder yawed  $45^\circ$ .



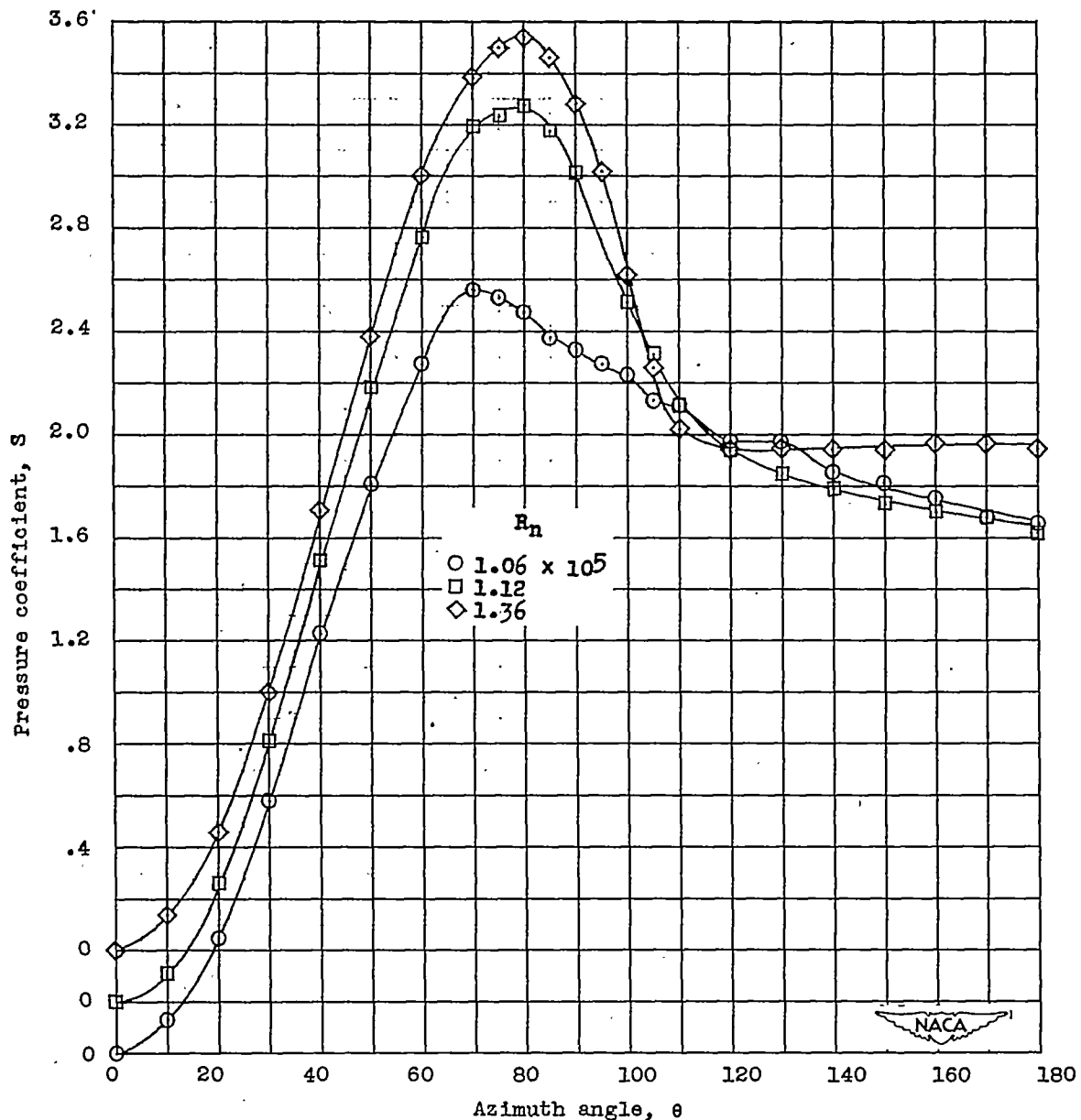
(b)  $R_n = 3.01 \times 10^5$  to  $R_n = 4.25 \times 10^5$ .

Figure 6.- Concluded.



(a)  $R_n = 0.60 \times 10^5$  to  $R_n = 1.02 \times 10^5$ .

Figure 7.- Circumferential pressure distributions at several Reynolds numbers of a 2-inch-diameter circular cylinder yawed  $60^\circ$ .



(b)  $R_N = 1.06 \times 10^5$  to  $R_N = 1.36 \times 10^5$ .

Figure 7.- Concluded.

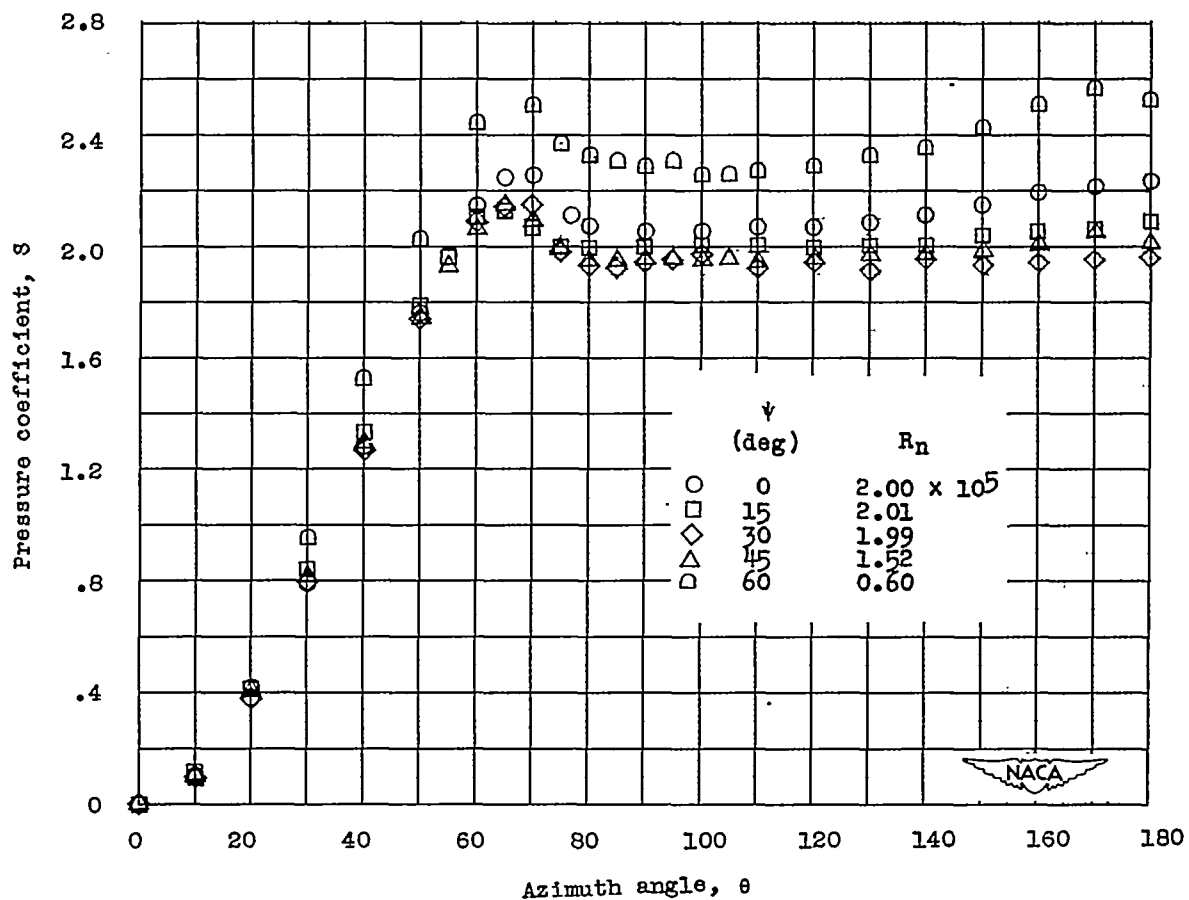


Figure 8.- Comparison of circumferential pressure distributions of a 2-inch-diameter circular cylinder at several yaw angles for Reynolds numbers in the subcritical range.

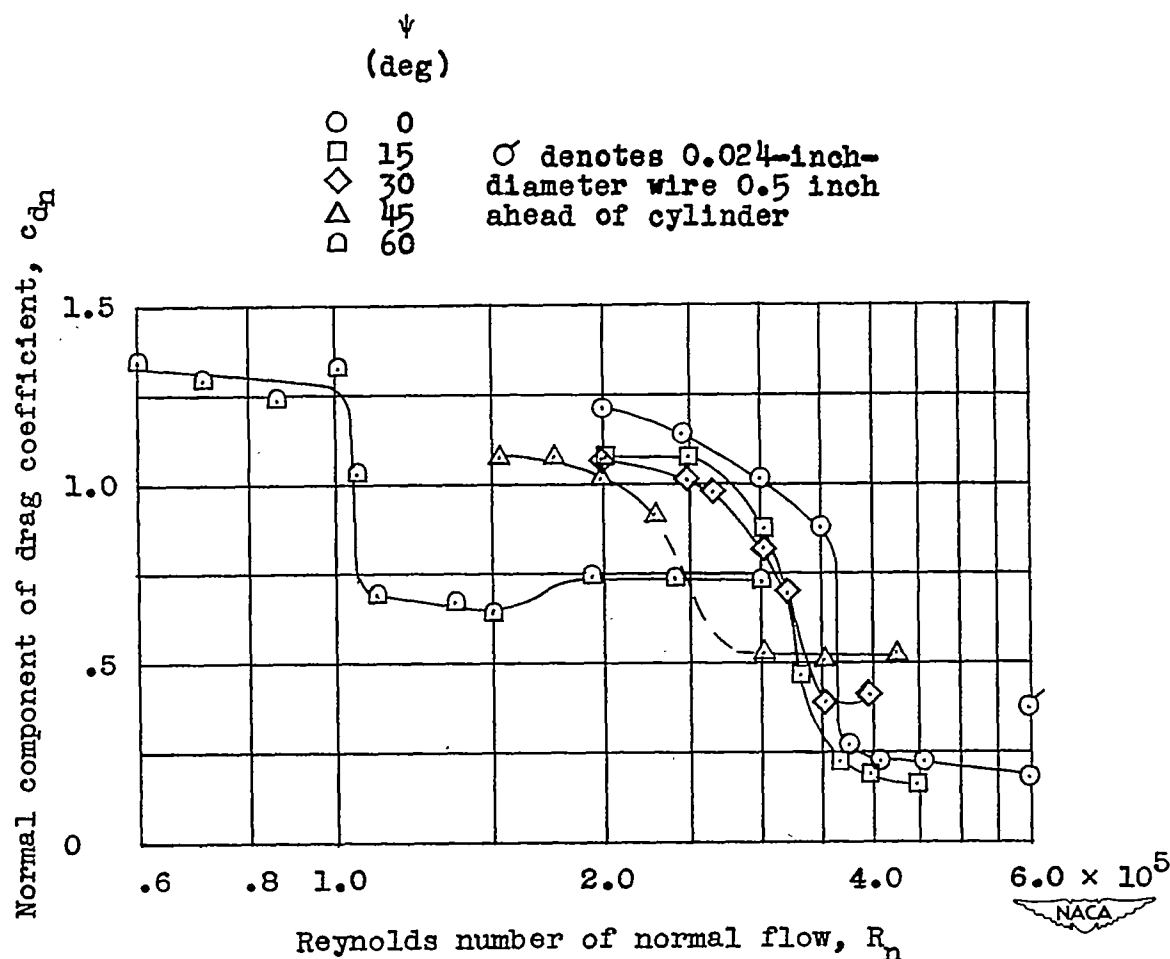


Figure 9.— Variation of drag coefficient with Reynolds number for a 2-inch-diameter circular cylinder at several angles of yaw. (Reynolds number is based on cylinder diameter and component of velocity normal to axis of the cylinder.)

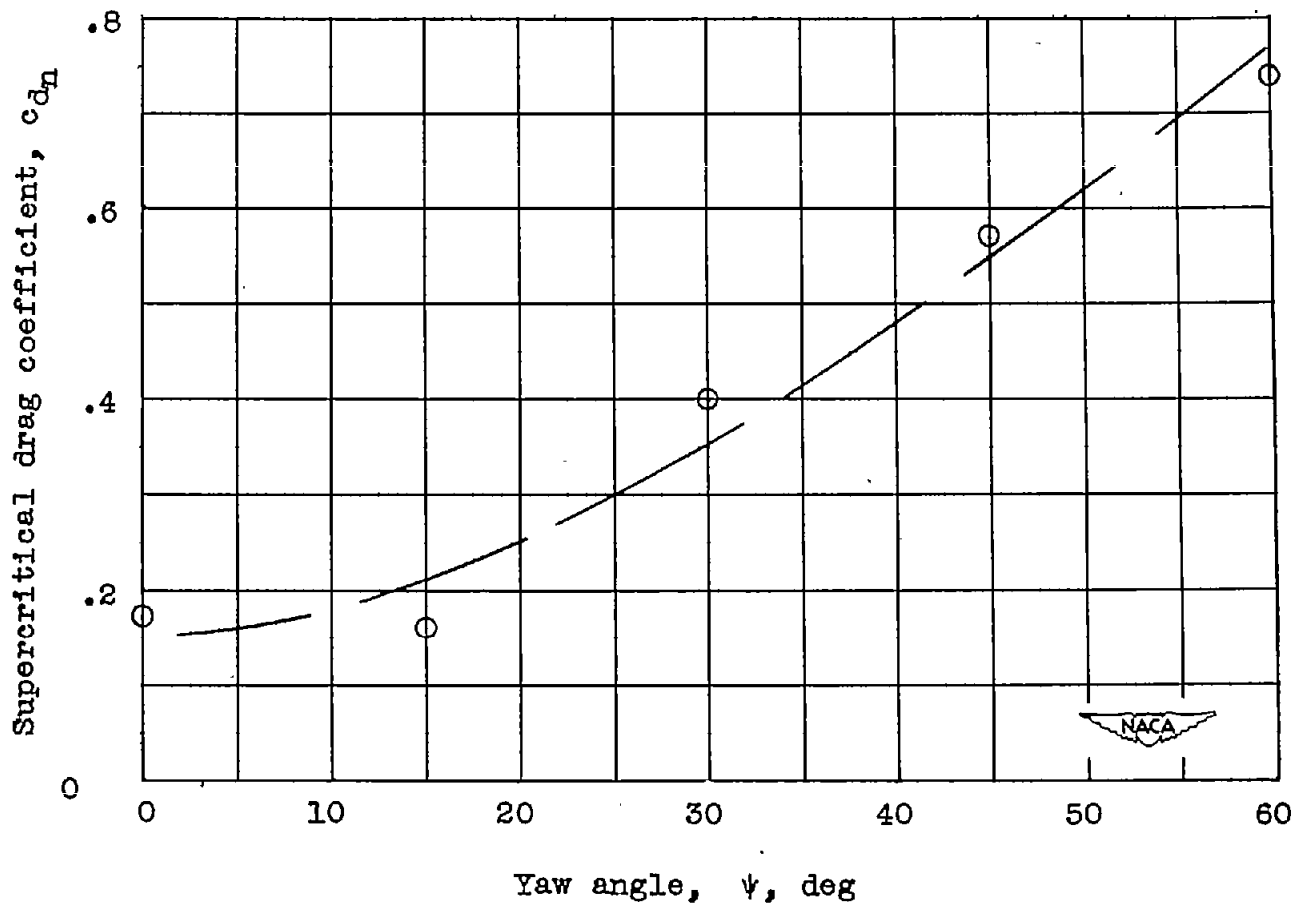


Figure 10.- Variation of supercritical drag coefficient with yaw angle for a 2-inch-diameter circular cylinder.